

Antiferromagnetic Coupling Across a Tetrametallic Unit Through Noncovalent Interactions

Eric W. Dahl,^a Frederick G. Baddour,^a Wesley A. Hoffert,^b Stephanie R. Fiedler,^b Matthew P. Shores,^b Gordon Yee,^c Jean-Pierre Djukic,^d Jeffrey W. Bacon,^a Arnold L. Rheingold,^e Linda H. Doerrer*,^a

^aDepartment of Chemistry, Boston University, Boston, MA 02215, United States

^bDepartment of Chemistry, Colorado State University, Fort Collins, CO, 80523, United States

^cChemistry Department, Virginia Tech, Blacksburg, VA, 24061, United States

^dCNRS, Institut de Chimie, 67000 Strasbourg, France

^eDepartment of Chemistry and Biochemistry, University of California, San Diego, La Jolla, CA 92093, United States

Syntheses.

General Considerations. K₂PtCl₄ was prepared using a combination of literature preparations. H₂PtCl₆ was prepared¹ from commercially obtained Pt metal and was converted to K₂PtCl₆ using a literature preparation.² K₂PtCl₄ was then synthesized from K₂PtCl₆ using literature methods.³ All other reagents were obtained commercially and were used without further purifications. [Ni₂(tba)₄(EtOH)] was prepared according the literature.⁴ All reactions were carried out in air under ambient conditions unless otherwise specified. UV-Vis data were collected with a Shimadzu UV-3600 spectrometer. ¹H NMR spectra for Evans method were recorded on a Varian 500 MHz spectrometer. Elemental analyses were performed by Quantitative Technologies Inc. (QTI, Whitehouse, NJ 08888).

[PtFe(tba)₄(H₂O)]·(acetone) (1): Compound **1** was prepared similarly to **3** until the addition of the first-row metal chloride using the amounts: NaHCO₃ (0.1834 g, 2.183 mmol), Htba (0.2873 g, 2.079 mmol), K₂PtCl₄ (0.2158 g, 0.520 mmol). A solution of FeCl₃·6H₂O (0.1405 g, 0.520 mmol) in ~15 mL H₂O was added dropwise to the reaction flask causing an immediate precipitation of a dark purple solid. The solution was then heated to 70°C for 30 min, which caused the dark purple solid to turn brown. The brown solid was filtered over celite, washed with H₂O, then dissolved in ~400 mL acetone forming a red solution. The volume of acetone was reduced to ~10 mL *in vacuo* creating a red solid that precipitated out of solution. Hexanes was added sparingly to force additional precipitation of the red solid. The solid was then filtered and dried *in vacuo*. The red material was redissolved in acetone and recrystallized with hexanes twice more to give a red microcrystalline powder with [PtFe(tba)₄(H₂O)]·(acetone) composition in 27% yield. Larger red crystals were grown from slow evaporation of acetone for X-ray

crystallography. Anal. calcd: C, 42.52; H 3.22; N 0.00 %. Found: C, 42.46; H, 2.96; N <0.05 %. UV-Vis (DMF) (λ_{max} , nm (ϵ_M , $\text{cm}^{-1} \text{M}^{-1}$)): 314(32,400), 484(920), 996(13). Evans method (DMF-d₇): 5.11 μ_B .

[PtCo(tba)₄(H₂O)]₂·5THF (2): Compound **2** was prepared similarly to **3** with the same amounts used until the addition of the first-row metal chloride. A solution of CoCl₂·6H₂O (0.2310 g, 0.843 mmol) in ~15 mL of H₂O was added dropwise to the reaction flask and let stir for 24 hours. The light green/beige precipitate that formed was separated from the colorless solution by filtering over celite. The powder was dissolved in THF and recrystallized with addition of hexanes to give a green powder with 64% yield. Yellow/light brown crystals of **2b** were grown from slow evaporation of CH₂Cl₂. Purple block-shaped crystals of **2a** were grown from slow evaporation of THF and found to have the [PtCo(tba)₄(H₂O)]₂·10THF composition. Recrystallization of the green/beige material from CH₂Cl₂ and hexanes was found to have the composition [PtCo(tba)₄(H₂O)] (**2b**). Anal. Calcd. (**2a**): C, 45.59; H, 4.23; N 0.00 %. Found: C, 45.49; H, 3.98; N <0.05 %. Anal. Calcd. (**2b**): C, 40.97; H, 2.70; N, 0.00 %. Found: C, 40.97; H, 2.73; N, 0.00 %. UV-Vis (THF) (λ_{max} , nm (ϵ_M , $\text{cm}^{-1} \text{M}^{-1}$)): 236(62,300), 295(30,500), 307(30,900), 495(28), 579(11), 1275(3). Evans method (DMF-d₇): 5.02 μ_B .

[PtNi(tba)₄(H₂O)]·THF (3): A solution of NaHCO₃ (0.2975 g, 3.541 mmol) in ~100 mL H₂O was added to Thiobenzoic Acid (Htba) (0.4661 g, 3.373 mmol) and swirled by hand at room temp without a stir bar. The solution turned light yellow after ~10 min and was then transferred to another flask – leaving behind any protonated Htba. The stir bar was then added. A solution of K₂PtCl₄ (0.3500 g, 0.843 mmol) in ~15 mL H₂O was added to the flask, let stir for 1-2 min, followed by the dropwise addition of a NiCl₂·6H₂O (0.2308 g, 0.843 mmol) solution in ~15 mL H₂O. Upon addition of the NiCl₂·6H₂O a slight clouding of the solution was observed. After stirring 24 hours, a yellow precipitate was separated from the colorless solution by filtering over celite. The yellow powder was dissolved in THF and recrystallized with addition of Hexanes in a 61% yield and found to have a [PtNi(tba)₄(H₂O)]·2THF composition. Anal. calcd: C, 44.82; H, 3.97; N 0.00 %. Found: C, 44.79; H, 3.78; N <0.05 %. Light green block-shaped crystals of **3** were grown from slow evaporation of THF for X-ray crystallography. After grinding and heating the crystalline powder to 90°C for 30 min, **3** was found to have the [PtNi(tba)₄(H₂O)]·THF composition. Anal. calcd: C, 43.06; H, 3.39; N 0.00 %. Found: C, 43.26; H, 2.92; N <0.05 %. Care was taken to use X-ray quality crystals in all solid-state measurements. UV-Vis (THF) (λ_{max} , nm (ϵ_M , $\text{cm}^{-1} \text{M}^{-1}$)): 246(56,300), 284(32,600), 321(27,700), 698(9), 820(6), 1337(10). Evans method (DMF-d₇): 3.11 μ_B .

Single Crystal X-ray Diffraction. A crystal of **2a** was mounted on a Cryoloop with Paratone-N oil and data was collected at 100 K with Cu $K\alpha$ radiation at 40 s/frame. Data were corrected for absorption with the SADABS program and structure was solved by direct methods. All non-hydrogen atoms were placed in calculated positions. S and O atoms were disordered over two positions (49.5/50.5) and were

modeled with DFIX commands for Co-O and C-O distances. Disorder (47.0/53.0) with respect to aromatic ring (C23-C28) was treated using a two part model with HFIX 66 restraint and EADP command for C24, C24A, C25, C25A. Residual electron density was treated using the Program Squeeze (found large void volume of 3874 Å³ with electron density of 1511 e⁻) this was associated with 38 (thirty-eight) THF molecules in the unit cell, consistent with the elemental analysis data.

An orange colored crystal of **2b** was mounted on a Cryoloop with Paratone-N oil. Data were collected on a Bruker APEX II CCD systems using Mo K α radiation in a nitrogen gas stream at 100(2) K using phi and omega scans. Crystal-to-detector distance was 60 mm and exposure time was 10 seconds per frame using a scan width of 0.5°. Indexing and unit cell refinement indicated a primitive, monoclinic lattice with space group *Pc*. Data was corrected for absorption by the program SADABS. Solution by direct methods (SHELXS) and all non-hydrogen atoms were refined anisotropically by full-matrix least-squares (SHELXL-97). All hydrogen atoms except those on the waters of hydration were placed in calculated positions with appropriate riding models. Hydrogen atoms on atoms O5 and O10 (waters of hydration) were found from a Fourier difference map, were restrained using DFIX and DANG commands and were allowed to refine. The structure was found to be twinned with a BASF ration of 72.4/27.6. CHECKCIF indicated a large solvent void but the residual electron density was centered around the Pt atoms and not in the void space.

DFT Calculations. All-electron, geometry-optimized, spin-unrestricted calculations were performed on [PtNi(tba)₄], [PtCo(tba)₄], and [PtFe(tba)₄] with idealized *C_{4v}* symmetry, and high-spin electron configurations in each, *S* = 1, 3/2, and 2 respectively, consistent with the experimental data. The expectation *S*² values for the three compounds are 6.06921 (PtFe), 3.75601 (PtCo), and 2.00553 (PtNi). In each case the origin was coincident with the 3d metal, the Pt-M vector coincident with the *z*-axis, and the *x*- and *y*-axes were aligned with the thiocarboxylate ligands. The 2010 version of ADF^{5, 6} was used including the GGA-BLYP functional, TZ2P basis sets for all atoms, and ZORA relativistic corrections for the Pt atoms. Frequency calculations on each of the three optimized structures showed genuine minima on the potential energy surface in the absence of any modes with negative frequencies. A comparison of the metal-ligand atom distances for the crystallographic and computational structures are collected in Table S3.

Spin-unrestricted and restricted calculations on *C₂* symmetry [PtM(tba)₄(OH₂)], M = Fe, Co, Ni, and *D₂* symmetry [PtM(tba)₄(OH₂)₂], M = Co, Ni, were carried out using the SCM ADF2010.2 package.^{5, 7} Gas-phase geometry optimizations were carried out by the energy gradient minimization method with tight SCF convergence criteria and integration accuracies spanning 4.5-6. Calculations were carried out using the GGA B⁸LYP⁹ functional and the dispersion-corrected GGA Perdew-Burke-Ernzerhof¹⁰(PBE-

D3¹¹) functional that includes Grimme's zero-damped third generation dispersion correction to the total bonding energy.¹² Within the PBE-D3 scheme electron correlation was treated within the local density approximation (LDA) in the PW92 parametrization.¹³ Within the BLYP scheme electron correlation was treated within the local density approximation (LDA) with the Vosko-Wilk-Nusair parametrization.¹⁴ Use of the PBE-D3 functional, a parent of the native PBE functional, was considered as a reasonable expedient¹⁵ to the modeling of the geometries of the paramagnetic lantern-type complexes and to a preliminary investigation of their electronic structure.¹⁶ Relativistic effects were treated in all cases with the ZORA formalism¹⁷ with recourse to ad-hoc all-electron triple- ζ polarized basis sets of Slater-type orbitals (STOs) for all elements including H.¹⁸ A comparison of the metal-ligand atom distances for the crystallographic and computational structures as well as the corresponding expectation values S^2 for the HS and BS states are collected in Table S3. The Gopinathan-Jug formalism¹⁹ was used for the geometries to compute two-atom bond indices (written n) with a value of 0.05 as threshold.

For monomers $[\text{PtNi}(\text{tba})_4 \cdot \text{H}_2\text{O}]$, $[\text{PtCo}(\text{tba})_4 \cdot \text{H}_2\text{O}]$ (**2b**), and $[\text{PtFe}(\text{tba})_4 \cdot \text{H}_2\text{O}]$ (**1**), spin-unrestricted geometry optimization was constrained to C_2 symmetry (principal z axis collinear with the metal-Pt axis) and to high-spin (HS) electron configurations $S = 1$ (spin polarization = 2), $3/2$ (spin polarization = 3), and 2 (spin polarization = 4) respectively, consistent with the experimental data at room temperature. For dimers $[\text{PtNi}(\text{tba})_4 \cdot \text{H}_2\text{O}]_2$ and $[\text{PtCo}(\text{tba})_4 \cdot \text{H}_2\text{O}]_2$, spin unrestricted geometry optimization was constrained to D_2 symmetry (main z axis bisecting perpendicularly the Pt-Pt segment) at high spin configuration with $S=1$ (spin polarization = 2) and 3 (spin polarization = 6) respectively.

The resulting geometries were used with no symmetry constraint to perform single point computations of low spin configurations of $[\text{PtNi}(\text{tba})_4 \cdot \text{H}_2\text{O}]$ ($S=0$), $[\text{PtCo}(\text{tba})_4 \cdot \text{H}_2\text{O}]$ ($S=1/2$), $[\text{PtNi}(\text{tba})_4 \cdot \text{H}_2\text{O}]_2$ ($S=0$) and $[\text{PtCo}(\text{tba})_4 \cdot \text{H}_2\text{O}]_2$ ($S=0$) by applying the "spin-flip" broken symmetry (BS) method.²⁰⁻²² In each case the high spin configuration was recomputed with no symmetry constraint with tight SCF convergence criteria. The resulting energy differences between the HS and BS configurations reproduced the trends established experimentally as to the relative stability of the low and the high spin states. However, as expected for large many-electrons systems treated within a GGA scheme,^{23, 24} the computed values of spin coupling constants J were found in all cases to be largely overestimated compared to those determined experimentally for solid-state samples; test computations carried out with the dispersion corrected meta-GGA functional TPSS²⁵ (i.e TPSS-D3^{11, 12}) led to only slightly improved energy differences²⁶ between HS and BS states. Kohn-Sham spin density polarizations in HS and BS states were materialized by subtracting β SCF spin density to α SCF spin density using ADFview2010. Other plots of the coulombic potential maps over SCF electron density and molecular orbital were also drawn using ADFview.

Analytical frequency calculations on each of the three water-free optimized structures in their high spin state were exempt of imaginary vibrational modes indicating that they were genuine minima on the potential energy surface. However, due to large symmetry constraints on the water molecule (of which the C_2 axis was virtually forced to remain colinear with the C_2 axis aligned on the M-Pt vector) and due to the repulsive tendency of the M-to-water interaction in the GGA structures of those water-containing complexes, calculations of normal vibrational modes produced systematically an imaginary eigenvalue associated essentially with the disruption of the M-to-water interaction ($M = \text{Fe, Co, Ni}$). This issue associated with the limitations inherent to the use of pure GGA functionals^{27, 28} was not addressed in this preliminary report. Computation of the HS and BS states of $[\text{PtNi(tba)}_4\cdot\text{H}_2\text{O}]$ at the UPBE^{29, 30}/AE-TZP level improved the description of the BS state by producing a neat $S=0$ state. However the J constant was still largely overestimated, which partly disqualifies this hybrid for the description of the magnetic behaviour of this series of complexes. Resorting to other hybrid functionals³¹ or to higher levels of theory in Jacob's ladder of methods (such as CI), with careful adjustment of the geometry of the adsorbed water molecule, should enable a better reproduction of those structural features and to a minimization of the delocalized nature of the electronic structure.

A spin restricted geometry optimization was also carried out with the C_2 -symmetric $[\text{PtNi(tba)}_4\cdot\text{H}_2\text{O}]_2$ ($S=0$) to probe the effect of the spin state over the Pt-Pt distance.

Diffuse Reflectance. Ultraviolet-visible (UV-vis) reflectance data were collected on a Varian Cary 500 scan UV-vis-NIR spectrophotometer over a spectral range of 200–2000 nm at room temperature. Poly(tetrafluoroethylene) was used as a reference material. Reflectance spectra were converted to absorbance data, using the Kubelka–Munk function.^{32, 33}

Magnetic Measurements. Magnetic susceptibility data were collected with a Quantum Design MPMS-XL SQUID magnetometer. For measurement between 2 and 300 K, samples were loaded into a gelatin capsule and inserted into drinking straws prior to analysis. Samples of **1** were measured as loosely-packed crystals as well as packed ground-up powders. The latter preparations show loss of solvate acetone, and data were interpreted accordingly.

Since compound **2a** decomposes upon grinding, a sample of purple crystalline blocks was left unground, and was measured as loosely-packed crystals and as crystals suspended in a matrix of eicosane to prevent torquing. Although the data are similar, given possible desolvation or reactions with hot eicosane, all data for **2a** are reported for crystals only. The crystals do not decompose during SQUID data collection. Data for **2b** were collected on light-yellow-colored powdered samples. Samples of **3** were measured in several different ways: as loosely-packed crystals, as crystals suspended in eicosane, as

packed ground-up powders, and as powders suspended in eicosane. The first three preparations provide qualitatively similar data. However, ground samples of **3** mixed with eicosane gave significantly different data and powder XRD measurements did not match predicted patterns, so data from this preparation was not analyzed further. For all measurements, diamagnetic corrections were applied by using Pascal's constants and by subtracting the diamagnetic susceptibility from the sample holder (including eicosane where appropriate). Where possible, susceptibility data were fit with theoretical models using a relative error minimization routine (julX 1.41).³⁴ Exchange coupling parameters are based on the Hamiltonian $\hat{H} = -2J(S_A \cdot S_B)$. Zero-field splitting parameters obtained with julX are based on the spin Hamiltonian:

$$\hat{H} = \sum D_i [S_{z,i}^2 - 1/3 S_i(S_i+1) + E_i/D_i (S_{x,i}^2 - S_{y,i}^2)] + \sum g\beta \vec{S}_i \cdot \vec{B}.$$

Fits of magnetization data were obtained with the ANISOFIT program³⁵ and are based on the Hamiltonian $\hat{H} = D\hat{S}_z^2 + E(\hat{S}_x^2 + \hat{S}_y^2) + g_{iso}\beta \vec{S} \cdot \vec{B}$. The MagSaki program³⁶ was used to simulate magnetic susceptibility data involving axially distorted Co(II)-containing compounds.

Table S1. Summary of X-ray crystallographic data collection parameters

Complex	1	2a	2b	3
Formula	C ₂₈ H ₂₂ FeO ₅ PtS ₄ , C ₃ H ₆ O	C ₄₇ H ₆₀ CoO _{9.75} PtS ₄	C ₂₈ H ₂₂ CoO ₅ PtS ₄	C _{32.35} H _{29.70} NiO _{6.09} PtS ₄
Formula weight	875.71	1163.21	820.72	897.95
Temp (K)	100(2)	100(2)	100(2)	293(2)
Crystal System	Monoclinic	Monoclinic	Monoclinic	Tetragonal
Space Group	<i>P</i> 2 ₁ / <i>n</i>	<i>I</i> 2/ <i>a</i>	<i>P</i> c	<i>I</i> 4̄ <i>c</i> 2
<i>a</i> (Å)	14.6379(6)	22.8140(8)	11.3784(7)	19.0697(15)
<i>b</i> (Å)	11.5625(5)	16.6711(7)	11.8220(8)	19.0697(15)
<i>c</i> (Å)	18.7162(8)	23.2989(14)	22.0722(14)	22.6005(19)
α (°)	90	90	90	90
β (°)	96.152(2)	92.135(2)	90.4290(10)	90
γ (°)	90	90	90	90
<i>V</i> (Å ³)	3149.5(2)	8855.2(7)	2969.0(3)	8218.8(11)
<i>Z</i>	4	8	4	8
ρ , calc. (Mg/m ³)	1.847	1.745	1.836	1.451
μ (MoK α), mm ⁻¹	14.721	11.013	5.583	9.052
Collected	37259	32723	25090	101221
Independent	5450	7410	12405	3586
<i>R</i> (int)	0.0540	0.0451	0.0256	0.0459
<i>R</i> (<i>F</i>), % ^a	2.85	4.34	2.79	3.34
<i>R</i> (ωF^2), % ^b	7.41	10.03	5.67	10.73

^a R=Σ||F_o|-|F_c||/ Σ|F_o| ^b R(ωF^2)={Σ[$\omega(F_o^2-F_c^2)^2$]/Σ[$\omega(F_o^2)^2$]}^{1/2}; $\omega=1/[\sigma^s(F_o^2)+(aP)^2+bP]$, P=[2F_c²+max(F_o,0)]/3

Table S2. Selected interatomic distances and angles for **1**, **2a**, **2b**, and **3**.

Complex		Distance (Å)		Angle (°)
1	Fe(1)-O(1)	2.099(2)	O(1)-Fe(1)-O(2)	91.49(9)
	Fe(1)-O(2)	2.062(2)	O(1)-Fe(1)-O(3)	172.49(10)
	Fe(1)-O(3)	2.125(2)	O(1)-Fe(1)-O(4)	90.24(9)
	Fe(1)-O(4)	2.102(2)	O(2)-Fe(1)-O(3)	88.39(9)
	Fe(1)-O(1W)	2.025(2)	O(2)-Fe(1)-O(4)	170.82(10)
	Pt(1)-S(1)	2.3333(8)	O(3)-Fe(1)-O(4)	88.73(9)
	Pt(1)-S(2)	2.3381(9)	O(5)-Fe(1)-Pt(1)	175.86(6)
	Pt(1)-S(3)	2.3136(8)	S(1)-Pt(1)-S(2)	90.28(3)
	Pt(1)-S(4)	2.3304(9)	S(1)-Pt(1)-S(3)	179.56(3)
	Fe(1)-Pt(1)	2.6319(6)	S(1)-Pt(1)-S(4)	90.33(3)
	O(1)-C(1)	1.247(4)	S(2)-Pt(1)-S(3)	90.10(3)
	O(2)-C(8)	1.245(4)	S(2)-Pt(1)-S(4)	179.17(3)
	O(3)-C(15)	1.248(4)	S(3)-Pt(1)-S(4)	89.30(3)
	O(4)-C(22)	1.259(4)		
	S(1)-C(1)	1.728(3)		
	S(2)-C(8)	1.724(3)		
	S(3)-C(15)	1.724(3)		
	S(4)-C(22)	1.710(3)		
2a	Co(1)-O(1)	2.099(10)	S(1A)-Pt(1)-S(2A)	89.98(12)
	Co(1)-O(2)	2.029(9)	S(1A)-Pt(1)-S(3A)	177.06(10)
	Co(1)-O(3)	2.069(8)	S(1A)-Pt(1)-S(4A)	111.4(2)
	Co(1)-O(4)	2.041(8)	S(2A)-Pt(1)-S(3A)	88.20(13)
	Co(1)-O(5)	2.031(4)	S(2A)-Pt(1)-S(4A)	158.6(2)
	Pt(1)-S(1A)	2.307(3)	S(3A)-Pt(1)-S(4A)	70.4(2)
	Pt(1)-S(2A)	2.355(3)	O(1)-Co(1)-O(2)	90.2(4)
	Pt(1)-S(3A)	2.352(3)	O(1)-Co(1)-O(3)	158.2(4)
	Pt(1)-S(4A)	2.355(3)	O(1)-Co(1)-O(4)	110.2(4)
	O(1)-C(1)	1.222(10)	O(2)-Co(1)-O(3)	68.3(4)
	O(2)-C(8)	1.276(10)	O(2)-Co(1)-O(4)	159.1(4)
	O(3)-C(15)	1.269(8)	O(3)-Co(1)-O(4)	91.1(4)
	O(4)-C(22)	1.281(10)	O(5)-Co(1)-Pt(1)	179.02(13)
	S(1A)-C(1)	1.678(5)	Co(1)-Pt(1)-Pt(1)	178.560(18)
	S(2A)-C(8)	1.673(5)		
	S(3A)-C(15)	1.678(6)		
	S(4A)-C(22)	1.743(6)		
	Co(1)-Pt(1)	2.5993(8)		
	Pt(1)-Pt(1)#1	3.0651(4)		
2b	Co(1)-O(1)	2.091(3)	O(1)-Co(1)-O(2)	89.12(13)
	Co(1)-O(2)	2.106(4)	O(1)-Co(1)-O(3)	177.18(13)
	Co(1)-O(3)	2.048(3)	O(1)-Co(1)-O(4)	90.10(14)
	Co(1)-O(4)	2.062(3)	O(2)-Co(1)-O(3)	91.40(14)
	Co(1)-O(5)	2.052(3)	O(2)-Co(1)-O(4)	178.32(13)
	Pt(1)-S(1)	2.3275(13)	O(3)-Co(1)-O(4)	89.31(14)
	Pt(1)-S(2)	2.3229(19)	O(5)-Co(1)-Pt(1)	177.39(10)
	Pt(1)-S(3)	2.3210(13)	S(1)-Pt(1)-S(2)	89.36(6)
	Pt(1)-S(4)	2.3187(18)	S(1)-Pt(1)-S(3)	178.75(5)
	O(1)-C(1)	1.270(5)	S(1)-Pt(1)-S(4)	90.20(6)
	O(2)-C(8)	1.257(6)	S(2)-Pt(1)-S(3)	91.44(6)
	O(3)-C(15)	1.248(5)	S(2)-Pt(1)-S(4)	179.51(7)
	O(4)-C(22)	1.258(6)	S(3)-Pt(1)-S(4)	89.01(6)
	S(1)-C(1)	1.706(5)	O(6)-Co(2)-O(7)	90.83(14)

	S(2)-C(8)	1.712(5)	O(6)-Co(2)-O(8)	177.19(13)
	S(3)-C(15)	1.714(5)	O(6)-Co(2)-O(9)	88.47(14)
	S(4)-C(22)	1.718(5)	O(7)-Co(2)-O(8)	90.88(15)
	Co(2)-O(6)	2.076(4)	O(7)-Co(2)-O(9)	178.35(12)
	Co(2)-O(7)	2.083(4)	O(8)-Co(2)-O(9)	89.76(14)
	Co(2)-O(8)	2.025(3)	O(10)-Co(2)-Pt(2)	176.80(11)
	Co(2)-O(9)	2.094(4)	S(5)-Pt(2)-S(6)	90.44(6)
	Co(2)-O(10)	2.035(3)	S(5)-Pt(2)-S(7)	179.45(7)
	Pt(2)-S(5)	2.3321(14)	S(5)-Pt(2)-S(8)	88.44(6)
	Pt(2)-S(6)	2.3286(19)	S(6)-Pt(2)-S(7)	90.08(6)
	Pt(2)-S(7)	2.3278(15)	S(6)-Pt(2)-S(8)	178.68(7)
	Pt(2)-S(7)	2.3131(19)	S(7)-Pt(2)-S(8)	91.04(6)
	O(6)-C(29)	1.264(5)		
	O(7)-C(36)	1.244(6)		
	O(8)-C(43)	1.253(5)		
	O(9)-C(50)	1.249(6)		
	S(5)-C(29)	1.709(5)		
	S(6)-C(36)	1.725(5)		
	S(7)-C(43)	1.726(5)		
	S(7)-C(50)	1.732(5)		
	Co(1)-Pt(1)	2.5521(5)		
3	Ni(1)-O(1)	2.055(7)	S(1)-Pt(1)-S(1A)	164.0(3)
	Ni(1)-O(1A)	2.10(3)	S(1)-Pt(1)-S(2)	89.94(9)
	Ni(1)-O(2)	1.995(9)	S(1)-Pt(1)-S(2A)	106.4(3)
	Ni(1)-O(2A)	2.03(4)	S(1A)-Pt(1)-S(2)	106.0(3)
	Ni(1)-O(3)	2.045(4)	S(1A)-Pt(1)-S(2A)	89.6(3)
	Pt(1)-S(1)	2.320(2)	S(2)-Pt(1)-S(2A)	163.5(2)
	Pt(1)-S(1A)	2.293(10)	O(1)-Ni(1)-O(1A)	163.3(7)
	Pt(1)-S(2)	2.334(2)	O(1)-Ni(1)-O(2)	88.6(3)
	Pt(1)-S(2A)	2.339(9)	O(1)-Ni(1)-O(2A)	104.5(10)
	O(1)-C(1)	1.272(9)	O(1A)-Ni(1)-O(2)	108.1(8)
	O(1A)-C(1)	1.26(3)	O(1A)-Ni(1)-O(2A)	92.2(12)
	O(2)-C(8)	1.268(11)	O(2)-Ni(1)-O(2A)	164.1(9)
	O(2A)-C(8)	1.19(4)	O(3)-Ni(1)-Pt(1)	180.00(5)
	S(1)-C(1)	1.696(6)	Ni(1)-Pt(1)-Pt(1)	179.998(4)
	S(1A)-C(1)	1.680(10)		
	S(2)-C(8)	1.713(6)		
	S(2A)-C(8)	1.679(10)		
	Ni(1)-Pt(1)	2.5649(10)		
	Pt(1)-Pt(1)	3.0816(5)		

Table S3. Comparison of crystallographic and computed gas-phase geometries in $[\text{PtM}(\text{tba})_4 \cdot \text{H}_2\text{O}]$ species

compound Method	1		[CoPt(tba)\cdotH₂O] (2b)		[NiPt(tba)\cdotH₂O]		2a		3			
	XRD	UPBE-D3 (C ₂)	XRD	UPBE-D3 (C ₂)	UPBE-D3 (C ₂)	XRD	UPBE-D3 (D ₂)	XRD	UPBE-D3 (D ₂)	UPBE (D ₂)	UPBE-D3 (D ₂)	
S M	2		3/2		1		3		1	1	0	
H ₂ O-M (Å)	2.025(2)	2.208	2.043(3)	2.193	2.138	2.031(4)	2.188	2.045(4)	2.208	2.239	2.332	
M-Pt (Å)	2.6319(6)	2.565	2.5521(5)	2.552	2.510	2.5993(8)	2.566	2.5649(10)	2.504	2.504	2.549	
S-Pt ^{a)} (Å)	2.3280(9)	2.371	2.322(2)	2.360	2.366	2.342(3)	2.365	2.321(5)	2.375	2.378	2.362	
O-M ^{a)} (Å)	2.097(2)	2.051	2.076(3)	2.046	2.030	2.059(9)	2.047	2.045 (5)	2.008	2.018	1.966	
O-M-Pt-S ^{a)} (deg)		15.3		19.4		20.4		19.7		19.2	18.8	17.2
Pt-Pt (Å)						3.0651(4)	3.089	3.0816(5)	2.931	2.981	2.971	
n _{M-Pt}	0.36		0.27		0.32		0.25		0.27		0.21	
n _{Pt-Pt}	-		-		-		<0.05		0.09		0.06	
n _{H₂O-M} ^{2 b)}	0.14		0.13		0.14		0.13		0.10			
S _{calc-HS} ^{2 b),c)}	6.055		3.764		2.007		12.026		2.543	2.032	1.48	
ρ _M ^{b)}	1.03		2.54		1.47		2.54		0.28			
ρ _{Pt} ^{b)}	-0.54		0.12		0.17		0.11		-0.07			
ρ _O ^{b)}	0.05		0.01		0.07		0.05		0.07			
Broken Symmetry												
S S _{calc-BS} ^{2 b)}			1/2		0		0		0			
(E _{HS} -E _{BS}) (kcal/mol)	-		1.064		1.002		2.974		1.781			
	-		-2.81		-10.83		+1.60		+8.19			

^{a)} average of four. ^{b)} computed with the symmetry constraint lifted. ^{c)} Mulliken-type spin densities; spin densities at S atoms were found negligible and are therefore not listed in this table.

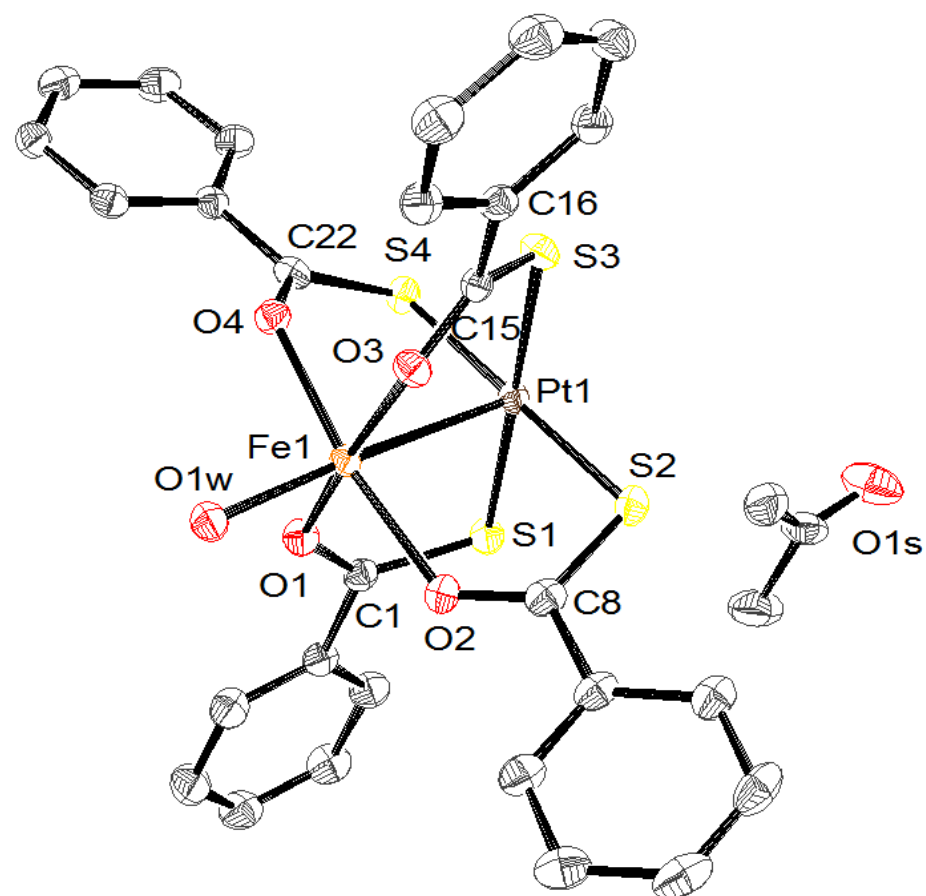


Figure S1. ORTEP of $[\text{PtFe}(\text{tba})_4(\text{OH}_2)] \cdot \text{acetone}$, **1**·acetone, with ellipsoids at 50% level and hydrogen atoms removed for clarity. Not shown are intermolecular $\text{Pt}(1)\dots\text{S}(3)$ contacts at $3.2596(9)$ Å.

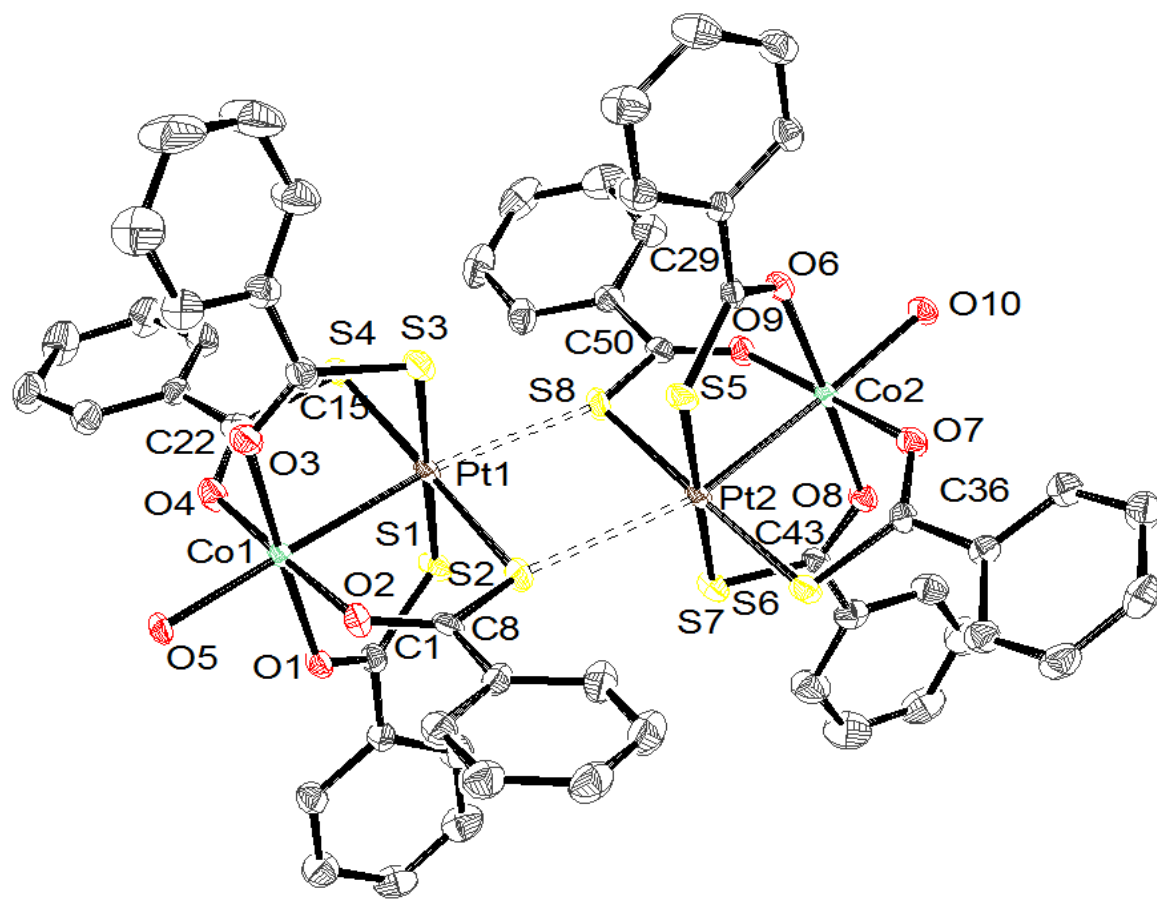


Figure S2. ORTEP of $[\text{PtCo}(\text{tba})_4(\text{OH}_2)]$, **2b**, with ellipsoids at 50% level and hydrogen atoms removed for clarity. The interdimer contacts are $2.978(1)$ Å for $\text{Pt}(1)\cdots\text{S}(8)$ and $3.106(1)$ Å for $\text{Pt}(2)\cdots\text{S}(2)$.

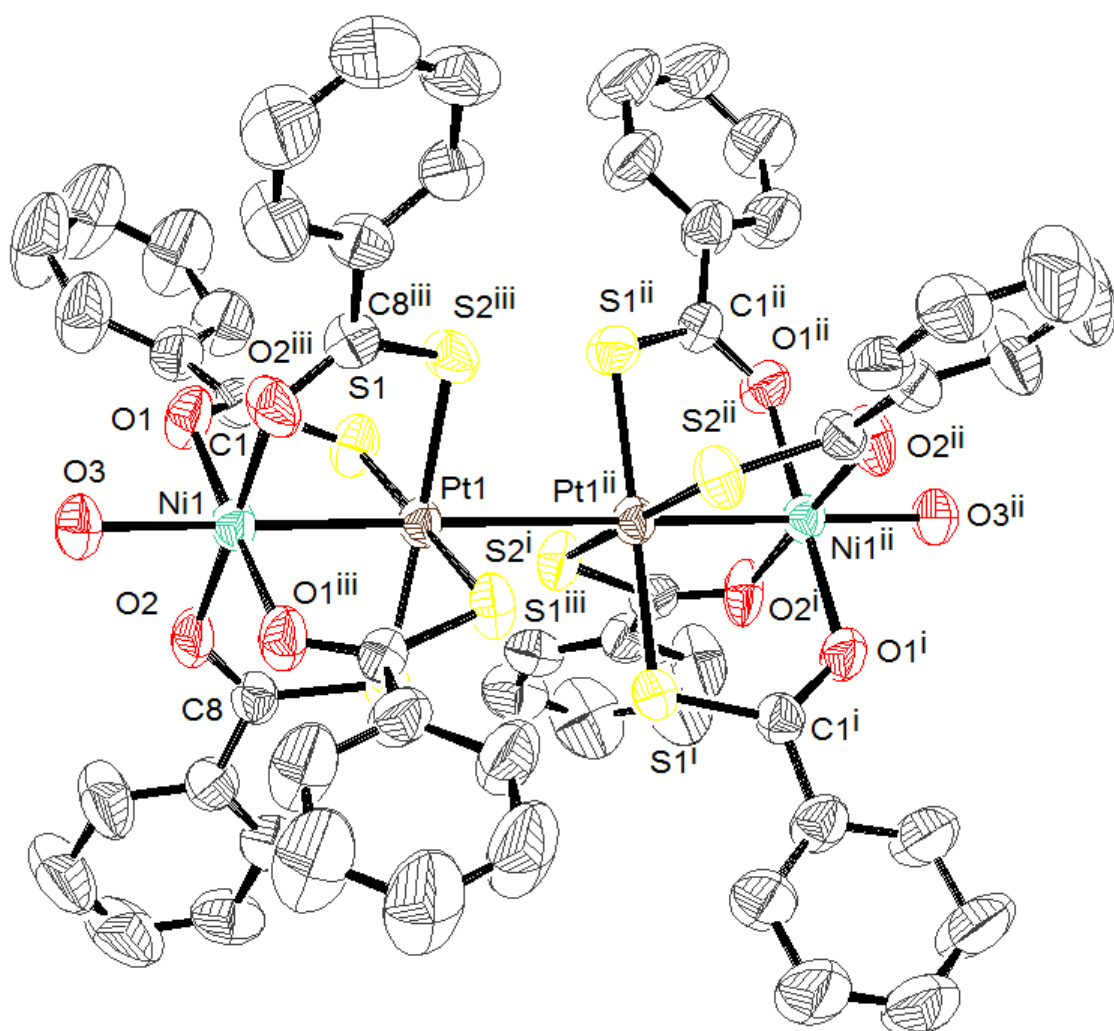


Figure S3. ORTEP of $[\text{PtNi}(\text{tba})_4(\text{OH}_2)]_2 \cdot \text{THF}$, **3**. Ellipsoids are at the 50% level. THF and hydrogen atoms have been removed for clarity.

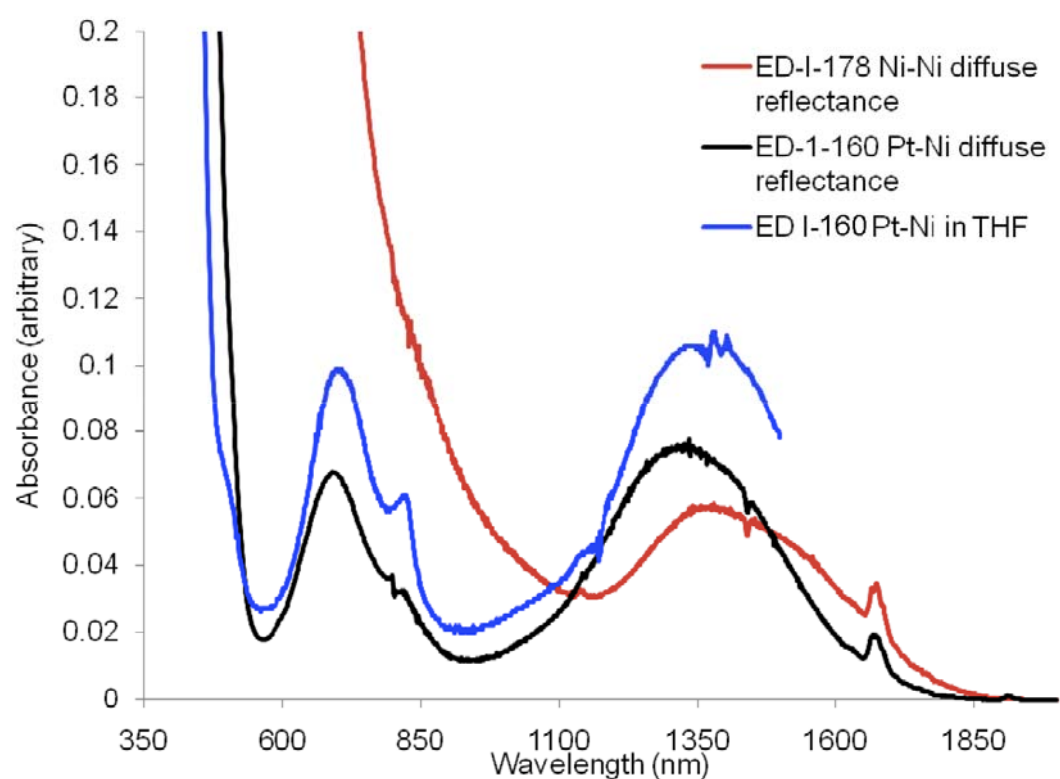


Figure S4. $[\text{Ni}_2(\text{tba})_4(\text{HOEt})]$ and $[\text{PtNi}(\text{tba})_4(\text{OH}_2)]$ in THF and in the solid state. The spectrum of $[\text{Ni}_2(\text{tba})_4(\text{HOEt})]$ was reported previously⁴ but was remeasured for comparison convenience.

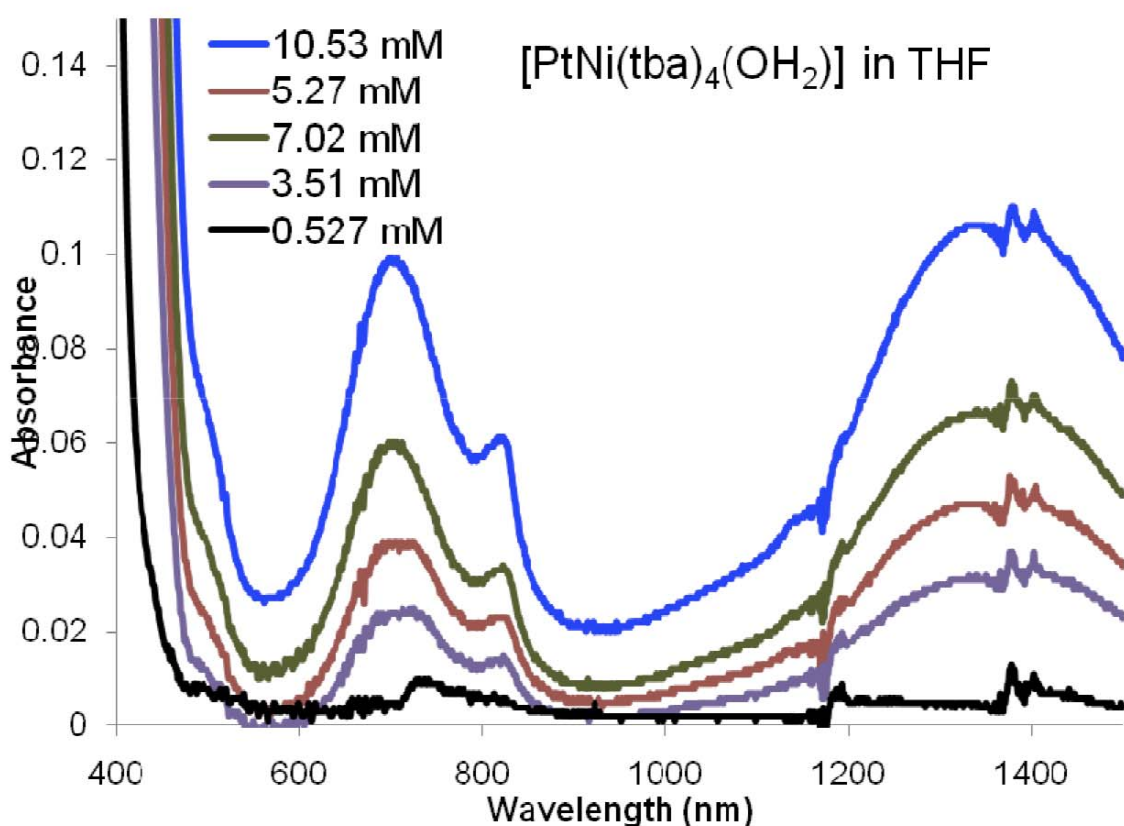


Figure S5. $[\text{PtNi}(\text{tba})_4(\text{OH}_2)]$, **3**, in THF at five different concentrations.

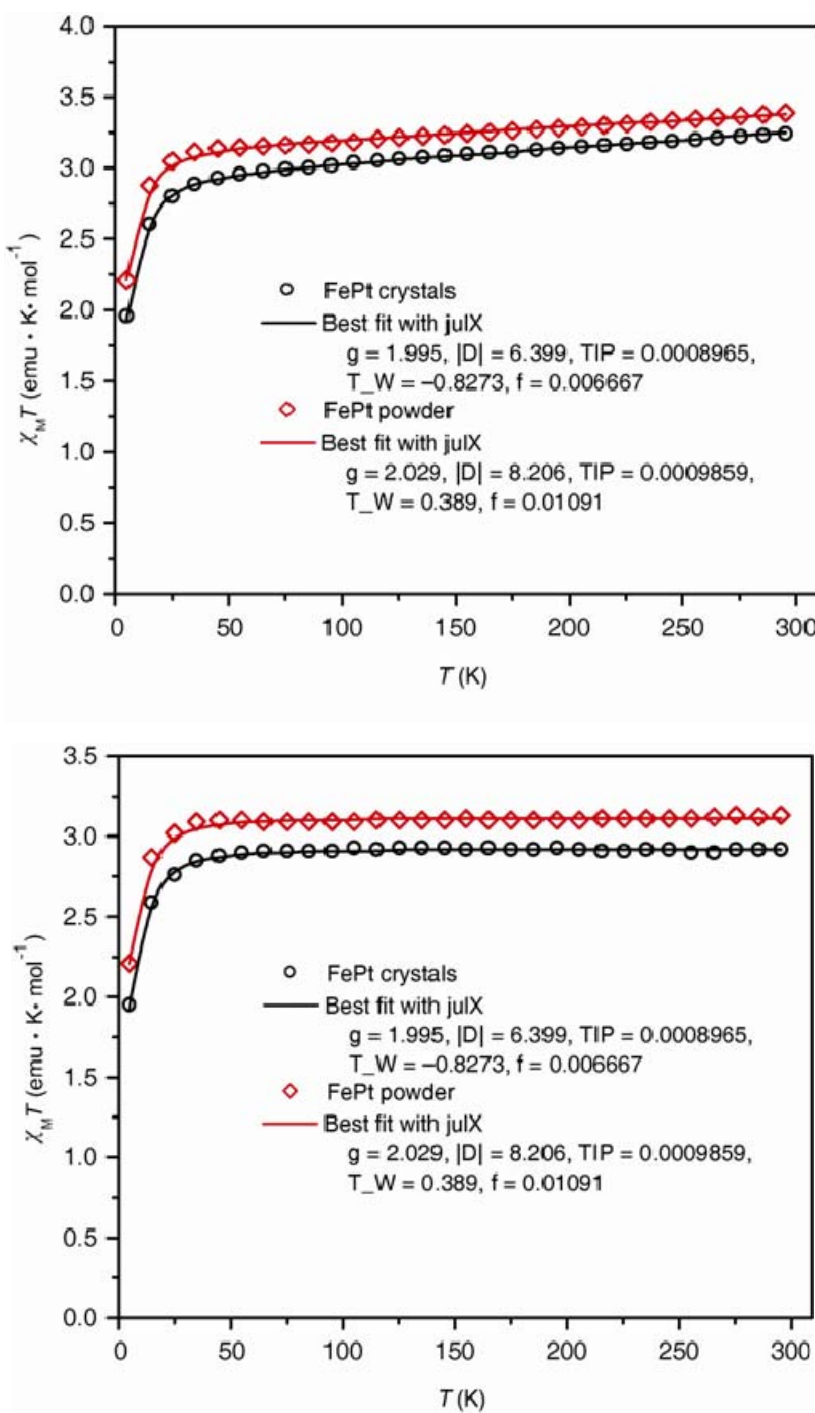


Figure S6. Temperature dependence of magnetic susceptibility for **1**, measured at 1000 G. Best fit parameters (via julX) are included in the figure with units of cm^{-1} for D and T_W (the mean field approximation to account for intermolecular interactions) and units of emu/mol for TIP. The raw data is shown in the top figure; the TIP contribution has been subtracted from the data shown in the bottom figure.

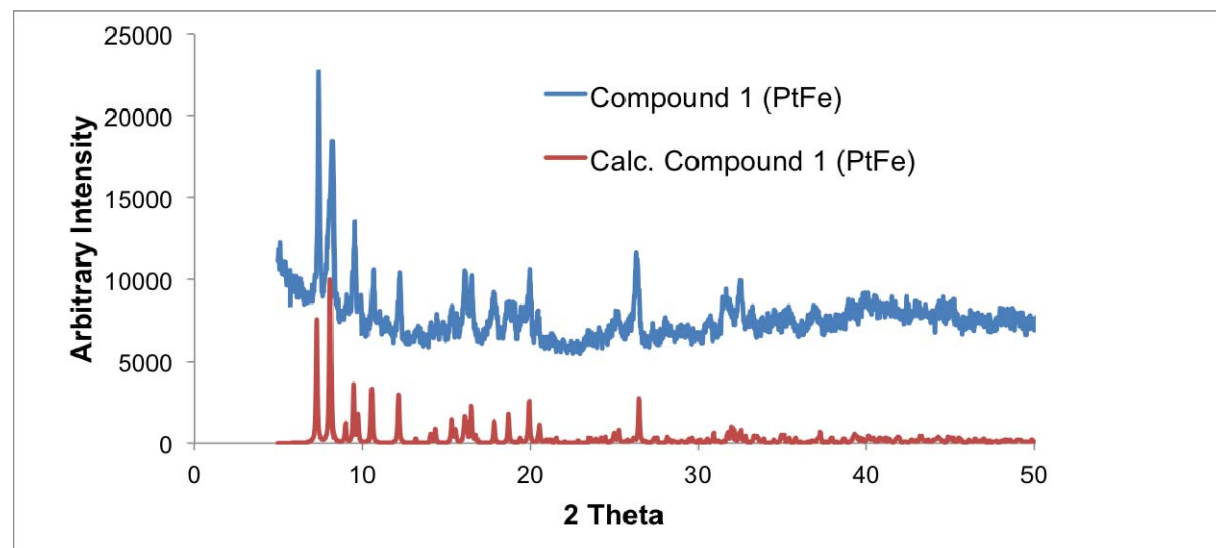


Figure S7. Comparison of experimental and calculated powder diffraction data for **1**.

Alternative fits and simulations for Co-containing complexes **2a and **2b**.** In the manuscript, we generate fits to the magnetic susceptibility data for **2a** and **2b** without including axial anisotropy (D) since $S = 0$ and $S = \frac{1}{2}$ states cannot have D (**2b** acts like $S = \frac{1}{2}$ at low temperature). However, since the spin Hamiltonian used by julX does not explicitly account for unquenched orbital angular momentum and/or spin-orbit coupling, commonly encountered with 6-coordinate Co(II) complexes, we attempted fits where we treat “ D ” simply as a parameter to be varied. For **2a**, including “ D ” results in nearly identical parameters and fit quality (Table S4).

Table S4. Comparison of julX-fitted magnetic parameters for **2a**.

	2a with no D (fit shown in manuscript)	2a with D
J (cm $^{-1}$)	-10.8	-10.8
g	2.15	2.14
D (cm $^{-1}$)	0	0.262
TIP (emu/mol)	3.47×10^{-3}	3.53×10^{-3}
mean-field approx. (cm $^{-1}$)	-6.4	-6.2
f	0.0335	0.0335

Alternative fitting scenarios for **2b** are shown in Table S5. Attempts to fit **2b** as a dimeric Co₂Pt₂ species yield unsatisfactory results. Tiny J values (intradimer coupling) in entries 1 and 2 support the assumption of minimal Co–Co magnetic interactions and the treatment of **2b** as a monomer. The fit shown for entry 3 is reasonably similar to the values obtained for **2a**. In fact, fits obtained with g and D values fixed to those found for **2a** (entry 4) also refine to similar values. Since the “ D ” value found for entry 3 was negligible, we concluded that reducing the number of parameters presented in the manuscript was warranted (entry 6). These fits include a mean field approximation in monomer and dimer cases: these are consistent with the intermolecular interactions observed in the solid-state crystal structure. Removal of the mean-field correction results in a “ D ” that is physically unreasonable (entry 5). In all cases large TIP values reflect the inability of the julX Hamiltonian to adequately model orbital contributions.

Table S5. Comparison of alternative fitted parameters for **2b**.

2b	(1)	(2)	(3)	(4)	(5)	(6)
	2b as dimer	2b as dimer, fix D & g to 2a fit	2b as monomer	2b as monomer, fix D & g values to 2a fit	2b as monomer, no MF correction	2b as monomer (fit in manuscript)
J (cm $^{-1}$)	0.055	0.007	n/a	n/a	n/a	n/a
g	2.18	2.14	2.18	2.14	2.17	2.18
D (cm $^{-1}$)	-1.394	0.262	0.002	0.262	43.41	n/a
TIP (emu/mol)	4.94×10^{-3}	5.581×10^{-3}	2.49×10^{-3}	2.784×10^{-3}	2.37×10^{-3}	2.49×10^{-3}
MF approx. (cm $^{-1}$)	-4.4	-3.7	-4.3	-3.7	n/a	-4.3
f	0.1183	0.1228	0.05889	0.06129	0.04998	0.05889

In an alternative fitting method, Sakiyama³⁷⁻⁴² and others^{38, 43, 44} have considered effects of ligand-field distortions on the magnetic behaviour of Co(II) ions. These systems can be modelled by accounting for the spin-orbit coupling (λ), axial ligand-field splitting (Δ), and an orbital reduction factor (κ). Results of these simulations are shown in Figure S10.

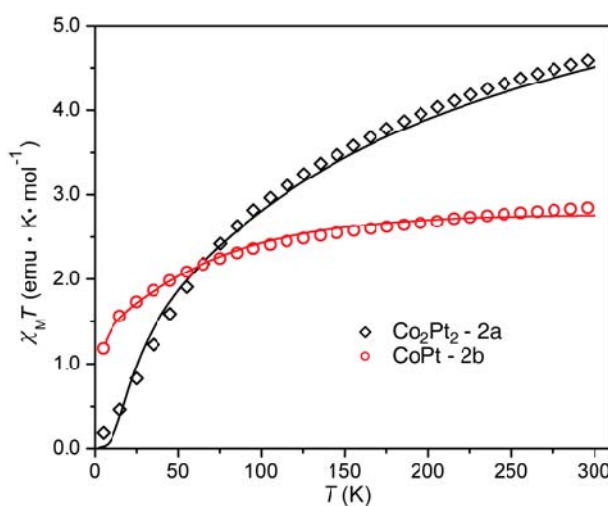


Figure S8. Results of MagSaki simulations for Co-containing complexes **2a** and **2b**. Solid lines are best fits obtained from MagSaki. The fit shown for **2a** has θ fixed to zero while the fit for **2b** has a freely-refined θ .

Simulating the **2b** data with MagSaki,³⁶ and fixing $S = 3/2$, $g = 2.0$, gives fitted parameters $\Delta = 351 \text{ cm}^{-1}$, $\kappa = 0.7$, $\lambda = -173 \text{ cm}^{-1}$, $\theta = -1.9 \text{ K}$, and $\text{TIP} = 1.21 \times 10^{-4} \text{ emu/mol}$. These values are typical for a Co(II) ion in an axially-distorted octahedral ligand field.³⁷ If we assume no intermolecular interactions (i.e. θ fixed to 0 K), similar parameters are obtained: $\text{TIP} = 0.001 \text{ emu/mol}$ (fixed), $\Delta = 658 \text{ cm}^{-1}$, $\kappa = 0.66$, and $\lambda = -173 \text{ cm}^{-1}$; note that Δ is larger and TIP refines to unreasonably small values, supporting the inclusion of θ .

An attempt was also made to simulate the magnetic data for **2a** using the axially distorted model that is built into MagSaki. Here, κ , λ , and Δ were obtained first by fitting the data above 100 K and then J was added to fit all the data. The large TIP value was necessary to reproduce the monotonic behaviour at higher temperatures: $g = 2.0$ (fixed), $\theta = 0 \text{ K}$ (fixed), $J = -11.6 \text{ cm}^{-1}$, $\text{TIP} = 4.4 \times 10^{-3} \text{ emu/mol}$, $\kappa = 0.92$, $\lambda = -172 \text{ cm}^{-1}$, $\Delta = 15.8 \text{ cm}^{-1}$. For comparison, refining the θ parameter results in similar values: $g = 2.0$ (fixed), $\theta = -11.11 \text{ K}$, $J = -11.1 \text{ cm}^{-1}$, $\text{TIP} = 4.6 \times 10^{-3} \text{ emu}$, $\kappa = 0.92$, $\lambda = -173 \text{ cm}^{-1}$, $\Delta = -15.9 \text{ cm}^{-1}$.

Lacking independent determinations of simulated values (e.g. g from EPR), the simulation is over-parameterized; nevertheless, the values obtained are consistent with a dinuclear complex containing axially-distorted Co(II) ions.⁴¹⁻⁴⁴

For the Co-containing complexes studied here, we find that the coupling between spin centers is rather weak, at least compared to the Ni-containing analogue **3**. Although structurally both **2a** and **2b** show intermolecular interactions in the solid state, the paths for possible magnetic exchange are significantly different, such that **2a** is best thought of as a $(\text{CoPt})_2$ species while **2b** acts more like a (CoPt) entity.

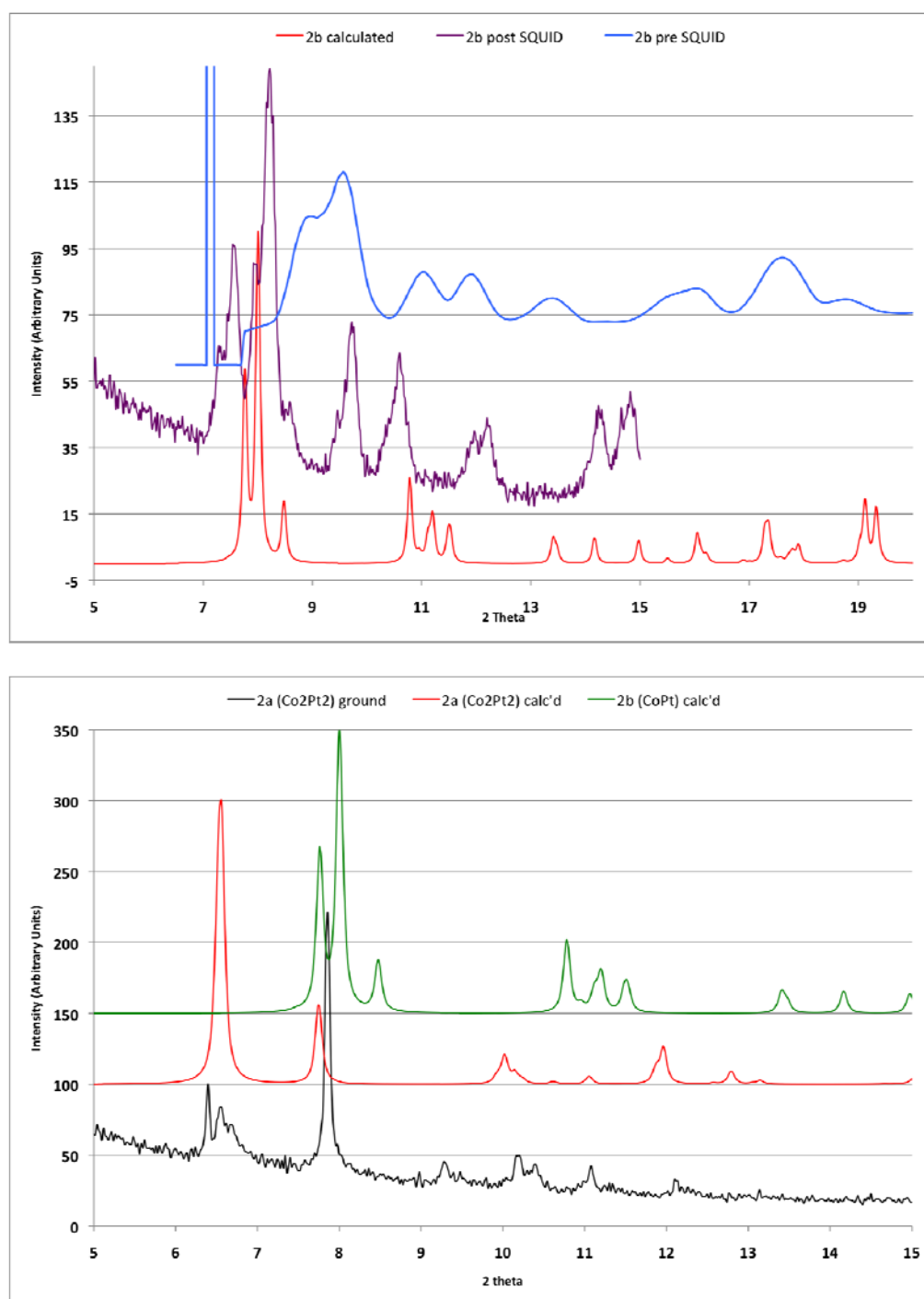


Figure S9. Comparison of calculated X-ray powder diffraction pattern for **2b** (red), pre-SQUID **2b** (blue), and compound **2b** after SQUID measurement (purple). Bottom: comparison of calculated X-ray powder diffraction for **2b** (green), calculated X-ray powder diffraction pattern for **2a** (red) and compound **2a** after grinding and SQUID measurement (black).

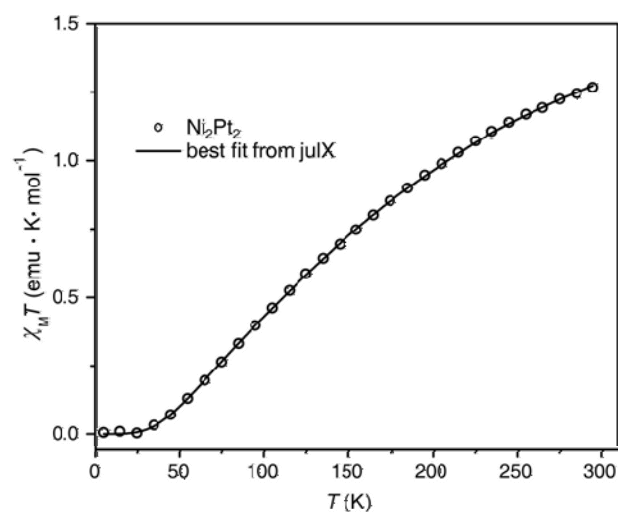


Figure S10. Temperature dependence of the magnetic susceptibility for ground crystals (powder) sample of **3**, measured in a 1000 G field. Best fit parameters (via julX) are provided in Table S6. Note: the TIP contribution has been subtracted from the data.

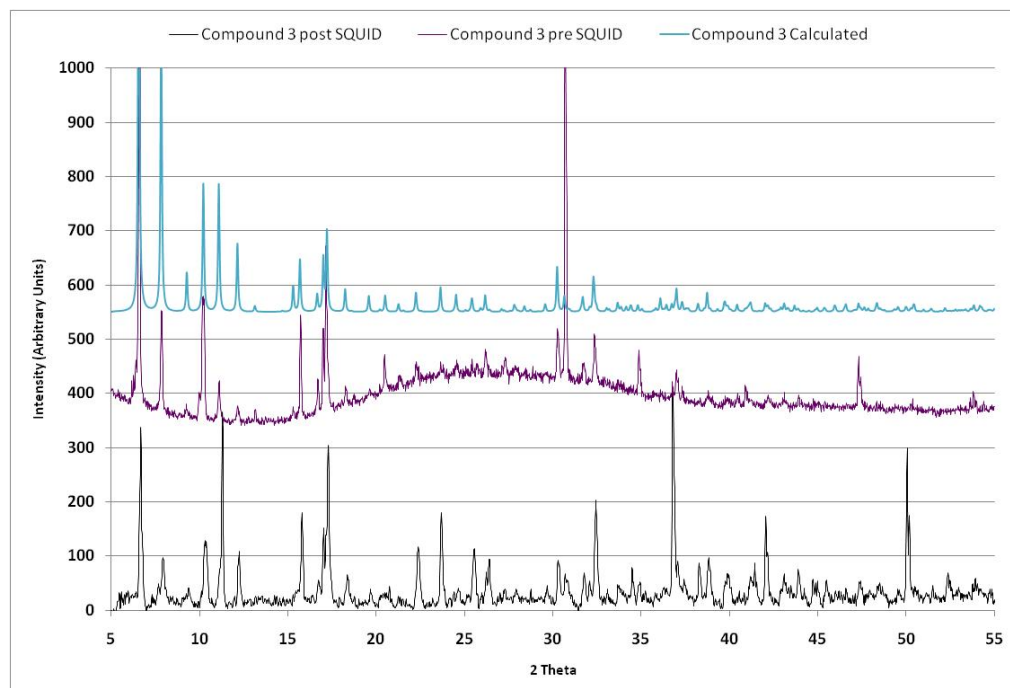


Figure S11. Comparison of calculated X-ray powder diffraction pattern for crystalline **3** (blue), powdered **3** before (purple), and after (black) SQUID measurement.

Table S6. Comparison of julX fits to the magnetic susceptibility data for **3**.

	3 powder	3 powder	3 crystals	3 crystals
J (cm $^{-1}$)	-58.34	-57.519	-59.683	-60.054
$g_1 = g_2$	2.039	1.999	2.187	2.193
TIP (emu/mol)	2.101×10^{-3}	2.222×10^{-3}	1.217×10^{-3}	1.217×10^{-3}
mean field approximation (cm $^{-1}$)	n/a	1.375	n/a	-0.585
f	0.003704	0.003661	0.003888	0.003785

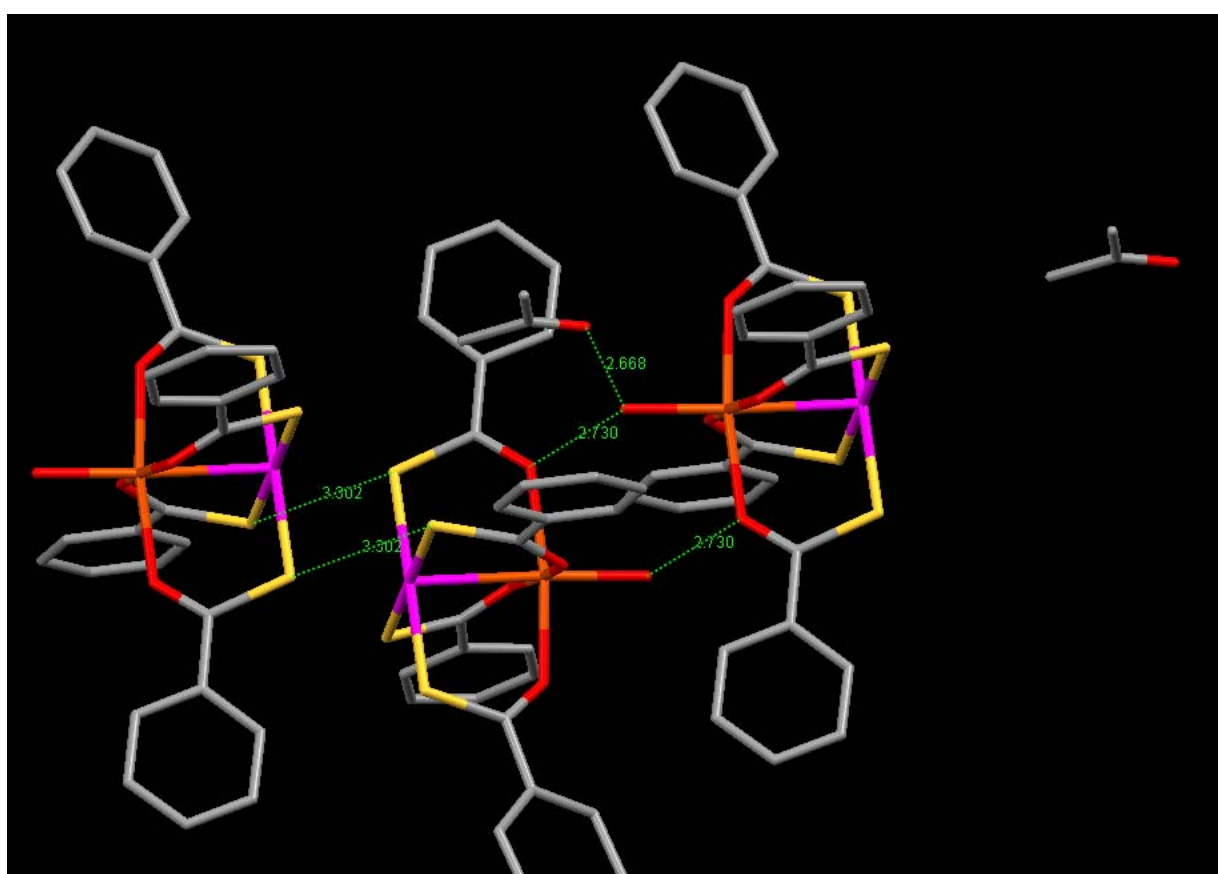


Figure S12. Hydrogen bonding interactions in the lattice of $[\text{PtFe}(\text{tba})_4(\text{OH}_2)]$, **1**, with distances shown in Ångstroms.

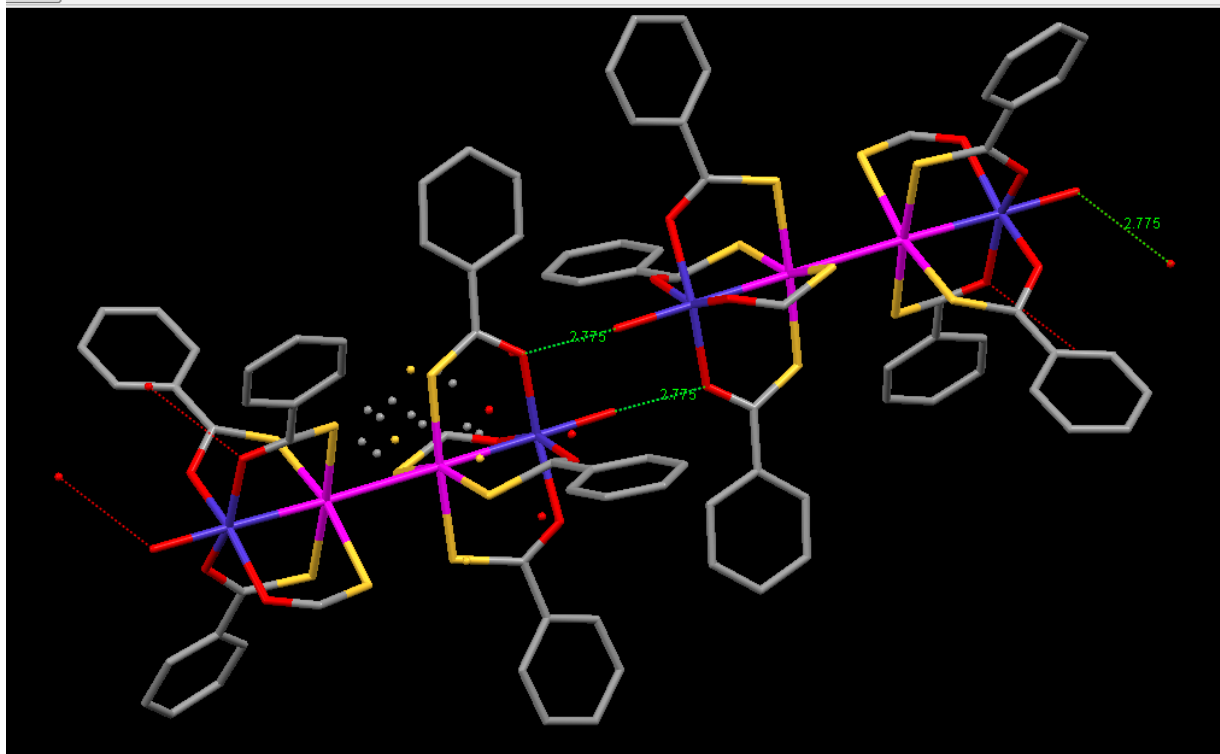


Figure S13. Hydrogen bonding interactions in the lattice of $[\text{PtCo}(\text{tba})_4(\text{OH}_2)]_2$, **2a**, with distances shown in Ångstroms.

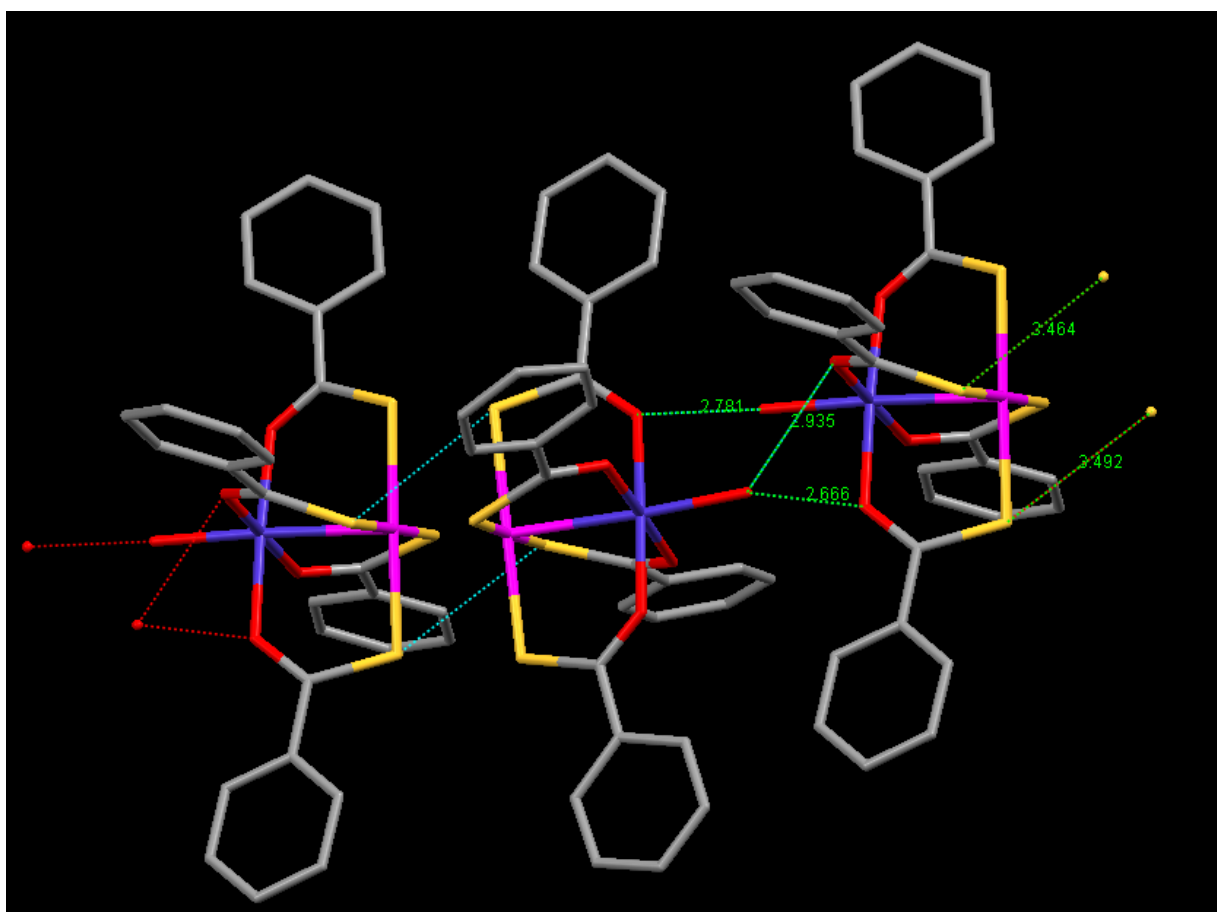


Figure S14. Hydrogen bonding interactions in the lattice of $[\text{PtCo}(\text{tba})_4(\text{OH}_2)]$, **2b**, with distances shown in Ångstroms.

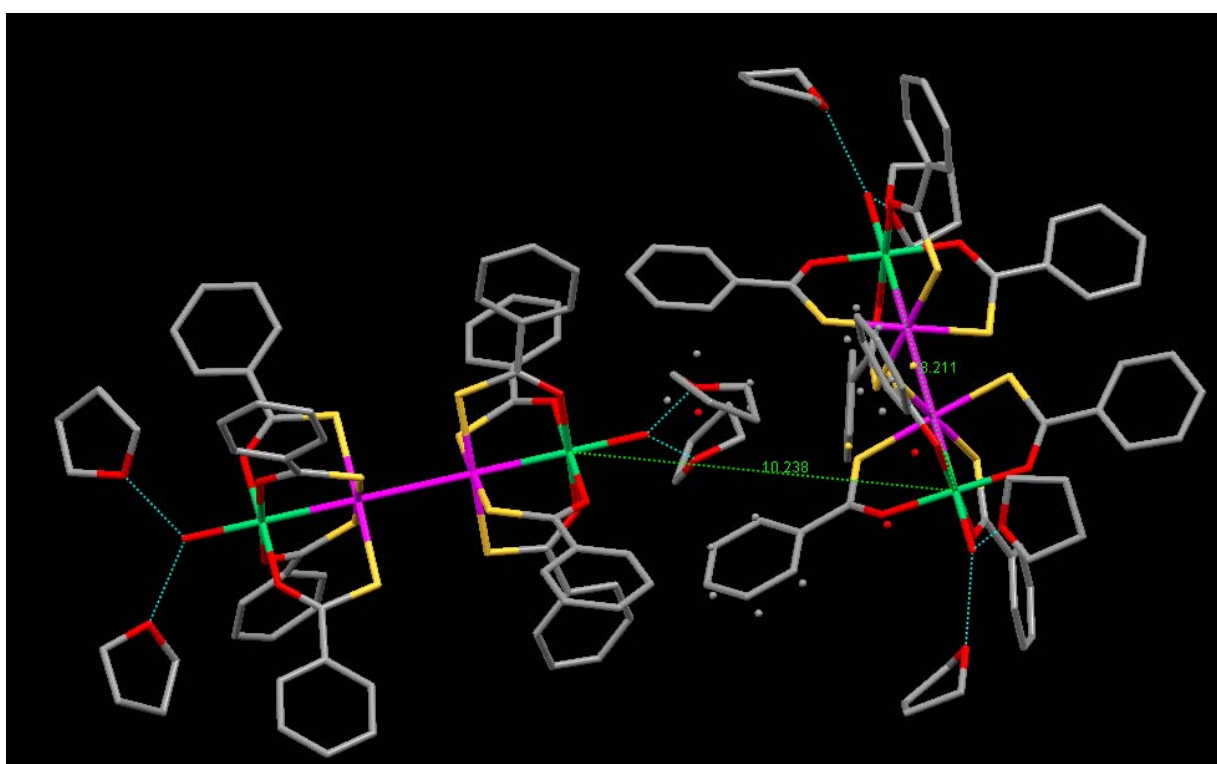


Figure S15. Hydrogen bonding interactions in the lattice of $[\text{PtNi}(\text{tba})_4(\text{OH}_2)]$, **3**, with distances shown in Ångstroms.

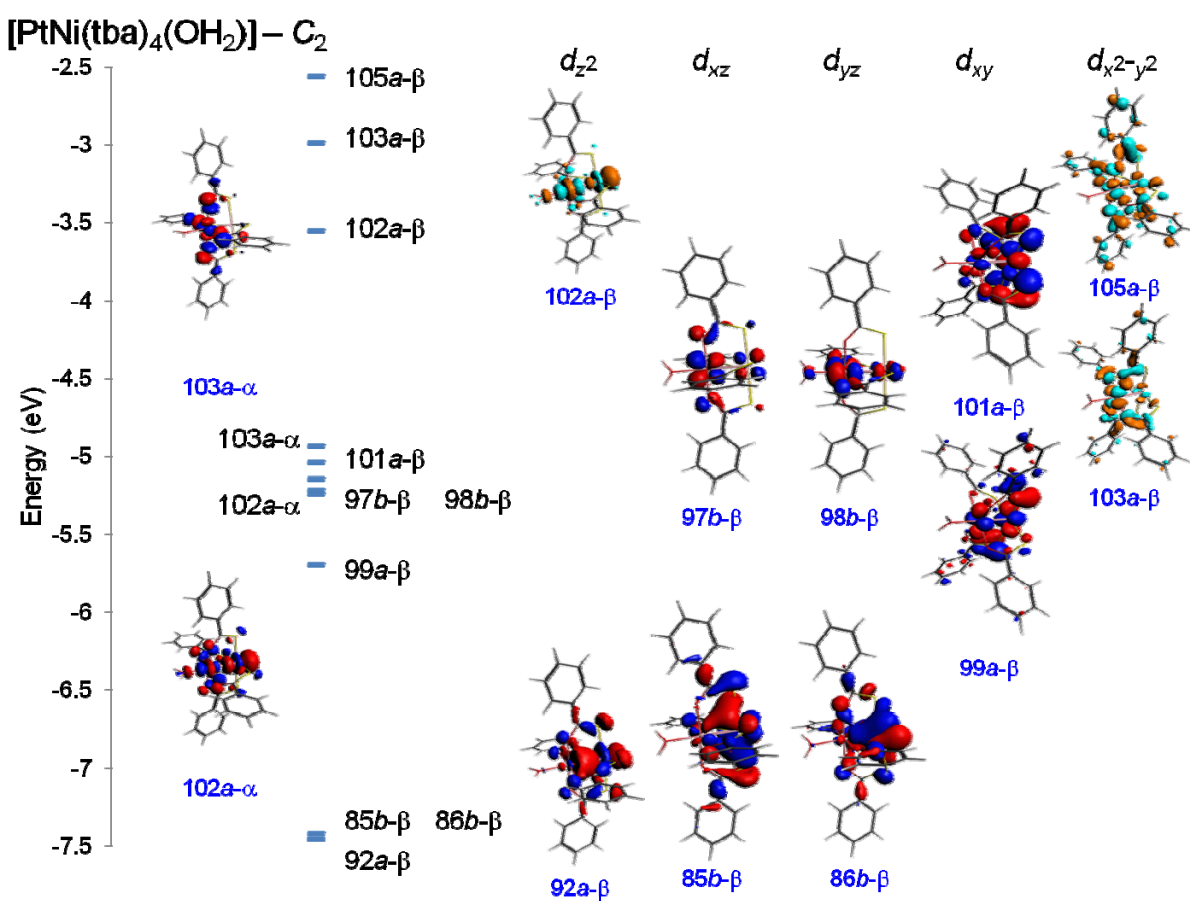


Figure S16. Energy level diagram and selected orbital pictures for DFT calculation of [PtNi(tba)₄(OH₂)] under C₂ symmetry.

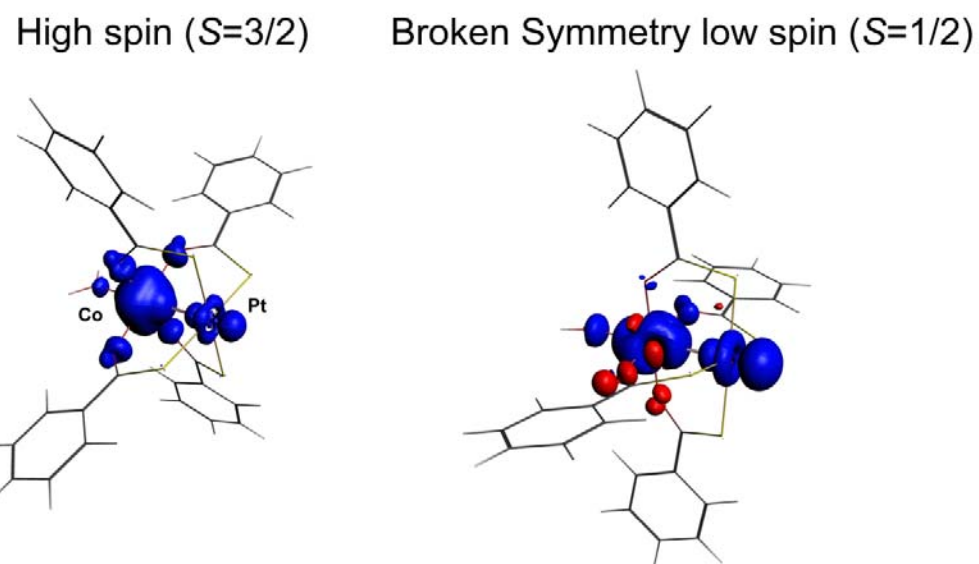


Figure S17. Isosurface plots ($0.005 \text{ e}/\text{\AA}^3$) of high spin and broken symmetry spin density polarizations in the $[\text{CoPt}(\text{tba})(\text{H}_2\text{O})]$ monomer (**2b**) as computed at the (ZORA) PBE-D3/AE-TZP level. Blue and red isosurfaces represent α and β spin domains respectively.

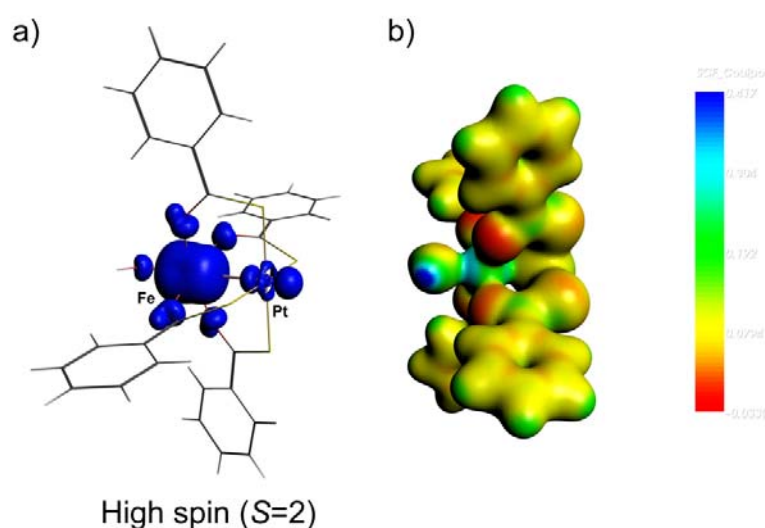


Figure S18. a) Isosurface ($0.005 \text{ e}/\text{\AA}^3$) plot of the spin density polarization (mostly α spins) for the high spin model of $[\text{FePt}(\text{tba})(\text{H}_2\text{O})]$ (**1**) computed at the (ZORA) UPBE/AE-TZP level. b) Coulombic potential (values comprised between -0.033 and 0.417 a.u.) map drawn over an isosurface ($0.03 \text{ e}/\text{\AA}^3$) of the total SCF electron density.

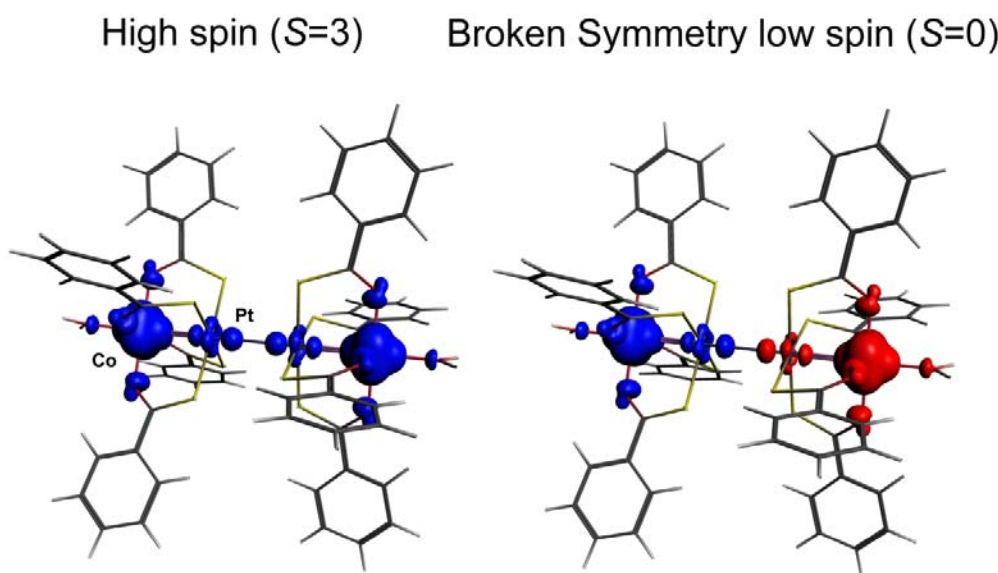


Figure S19. Isosurface plots ($0.005 \text{ e}/\text{\AA}^3$) of high spin and broken symmetry “low spin” spin density polarization in the model of **2a** as computed at the (ZORA) UPBE-D3/AE-TZP level. Blue and red isosurfaces represent α and β spin domains respectively.

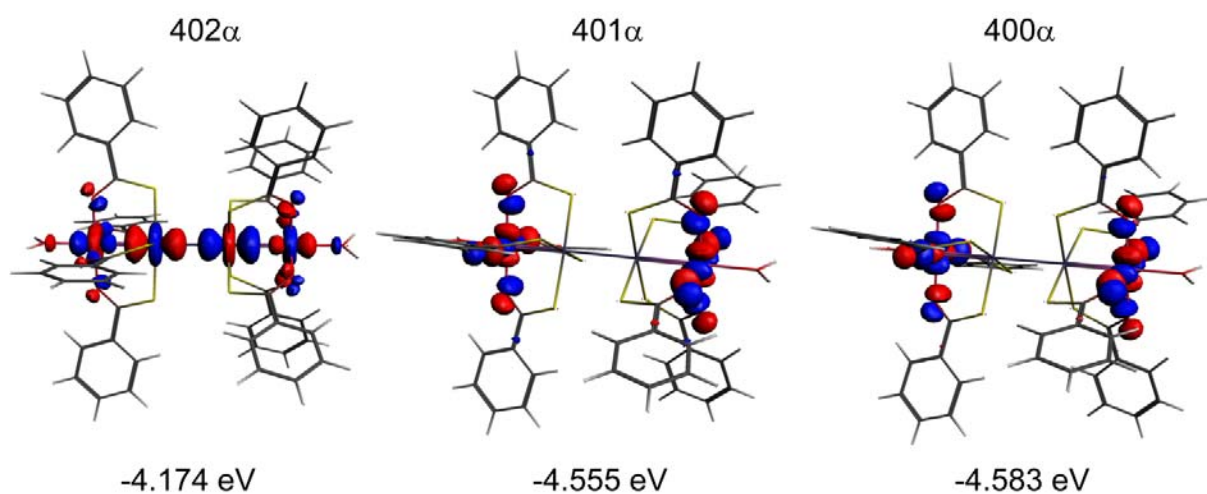


Figure S20. Plots of the singly occupied spin α molecular orbitals for the high spin model of **2a** computed at the (ZORA) UPBE-D3/AE-TZP level.

Computational part : Coordinates and energies

1, (ZORA)PBE-D3/AE-TZP, C2 symmetry

Atom	Cartesian (a.u./angstrom)		
	X	Y	Z
1 Pt	0.000000	0.000000	-0.000632
2 Fe	0.000000	0.000000	0.000100
3 C	0.000253	0.000037	-0.000048
4 H	-0.000169	-0.000019	0.000207
5 C	0.000067	-0.000296	0.000012
6 H	0.000139	0.000115	-0.000036
7 S	-0.000056	-0.000006	0.000008
8 S	0.000056	0.000006	0.000008
9 S	0.000146	-0.000099	0.000297
10 S	-0.000146	0.000099	0.000297
11 O	-0.000435	-0.000221	-0.000170
12 O	0.000435	0.000221	-0.000170
13 O	-0.000111	-0.000181	0.000114
14 O	0.000111	0.000181	0.000114
15 C	-0.000081	-0.000027	0.000250
16 H	-0.000213	0.000213	0.000045
17 C	0.000002	-0.000194	-0.000116
18 C	0.000116	-0.000372	-0.000133
19 H	0.000117	0.000067	-0.000321
20 C	0.000073	-0.000103	-0.000093
21 H	-0.000300	0.000199	-0.000007
22 C	-0.000073	0.000103	-0.000093
23 H	0.000300	-0.000199	-0.000007
24 C	-0.000032	0.000080	0.000034
25 H	0.000160	-0.000014	-0.000097
26 C	-0.000085	0.000034	0.000068
27 C	-0.000204	0.000105	0.000080
28 H	-0.000039	-0.000105	-0.000046
29 C	0.000134	-0.000016	-0.000241
30 C	0.000010	0.000026	-0.000150
31 H	-0.000001	0.000107	0.000238
32 C	0.000149	-0.000192	-0.000063
33 H	-0.000048	0.000126	0.000092
34 C	-0.000212	-0.000037	-0.000019
35 C	0.000081	0.000027	0.000250
36 H	0.000213	-0.000213	0.000045
37 C	0.000204	-0.000105	0.000080
38 H	0.000039	0.000105	-0.000046
39 C	-0.000134	0.000016	-0.000241
40 C	-0.000033	0.000208	-0.000169
41 H	-0.000219	-0.000175	-0.000033
42 C	0.000085	-0.000034	0.000068
43 C	-0.000116	0.000372	-0.000133
44 H	-0.000117	-0.000067	-0.000321
45 C	-0.000002	0.000194	-0.000116
46 C	-0.000253	-0.000037	-0.000048
47 H	0.000169	0.000019	0.000207
48 C	-0.000010	-0.000026	-0.000150
49 H	0.000001	-0.000107	0.000238
50 C	-0.000149	0.000192	-0.000063
51 H	0.000048	-0.000126	0.000092
52 C	-0.000067	0.000296	0.000012
53 H	-0.000139	-0.000115	-0.000036
54 C	0.000033	-0.000208	-0.000169
55 H	0.000219	0.000175	-0.000033
56 C	0.000032	-0.000080	0.000034
57 H	-0.000160	0.000014	-0.000097
58 C	0.000212	0.000037	-0.000019
59 O	0.000000	0.000000	0.000628
60 H	-0.000949	-0.000897	0.000249
61 H	0.000949	0.000897	0.000249

Geometry Convergence Tests

Energy old : -14.60448552
new : -14.60463947

Convergence tests:

(Energies in hartree, Gradients in hartree/angstr or radian, Lengths in angstrom, Angles in degrees)

Item	Value	Criterion	Conv.	Ratio	
					hartree eV kcal/mol kJ/mol
change in energy	-0.00015395	0.00100000	YES	1.92422276	
gradient max	0.00095264	0.00100000	YES	0.62391778	
gradient rms	0.00020995	0.00066667	YES	0.82363976	
cart. step max	0.00757537	0.01000000	YES	0.87665214	
cart. step rms	0.00194304	0.00666667	YES	1.13731089	
<hr/>					
Pauli Repulsion					
Kinetic (Delta T^0):	163.112534806663177		4438.5179	102354.67	428251.90
Delta V^Pauli Coulomb:	-83.736029161362097		-2278.5733	-52545.16	-219848.91
Delta V^Pauli LDA-XC:	-20.572346471456100		-559.8020	-12909.34	-54012.69
Delta V^Pauli GGA-Exchange:	1.057542624049994		28.7772	663.62	2776.58
Delta V^Pauli GGA-Correlation:	-0.241036373702133		-6.5589	-151.25	-632.84
Total Pauli Repulsion:	59.620665424192836		1622.3609	37412.54	156534.03
(Total Pauli Repulsion = Delta E^Pauli in BB paper)					
<hr/>					
Steric Interaction					
Pauli Repulsion (Delta E^Pauli):	59.620665424192836		1622.3609	37412.54	156534.03
Electrostatic Interaction:	-12.662985058465141		-344.5774	-7946.14	-33246.66
(Electrostatic Interaction = Delta V_elstat in the BB paper)					
Total Steric Interaction:	46.957680365727697		1277.7835	29466.39	123287.37
(Total Steric Interaction = Delta E^0 in the BB paper)					
<hr/>					
Orbital Interactions					
A:	-30.971375661248349		-842.7740	-19434.83	-81315.34
B:	-30.535170113872397		-830.9043	-19161.11	-80170.08
Total Orbital Interactions:	-61.512041770560394		-1673.8278	-38599.39	-161499.84
<hr/>					
Alternative Decomposition Orb.Int.					
Kinetic:	-148.640438020361046		-4044.7121	-93273.29	-390255.41
Coulomb:	80.799236015258870		2198.6591	50702.29	212138.36
XC:	6.329160234541757		172.2252	3971.61	16617.21
Total Orbital Interactions:	-61.512041770560415		-1673.8278	-38599.39	-161499.84
<hr/>					
Residu (E=Steric+OrbInt+Res):	-0.000035144328638		-0.0010	-0.02	-0.09
Dispersion Energy:	-0.050267508424341		-1.3678	-31.54	-131.98
Total Bonding Energy:	-14.604664057585676		-397.4131	-9164.57	-38344.54
<hr/>					
Summary of Bonding Energy (energy terms are taken from the energy decomposition above)					
Electrostatic Energy:	-12.662985058465141		-344.5774	-7946.14	-33246.66
Kinetic Energy:	14.472096786302131		393.8058	9081.38	37996.48
Coulomb (Steric+OrbInt) Energy:	-2.936828290431862		-79.9152	-1842.89	-7710.64
XC Energy:	-13.426679986566484		-365.3586	-8425.37	-35251.74
Dispersion Energy:	-0.050267508424341		-1.3678	-31.54	-131.98
Total Bonding Energy:	-14.604664057585696		-397.4131	-9164.57	-38344.54

2b, (ZORA) PBE-D3/AE-TZP, C₂ symmetry

Atom	Cartesian (a.u./angstrom)		
	X	Y	Z
1 C	0.000125	0.000123	-0.000104
2 C	-0.000031	-0.000023	0.000127
3 C	-0.000058	-0.000038	-0.000003
4 H	0.000009	0.000075	-0.000015
5 C	0.000015	0.000065	-0.000039
6 H	-0.000037	0.000043	-0.000049
7 C	0.000009	-0.000018	-0.000018
8 H	-0.000056	-0.000016	-0.000040
9 C	-0.000040	-0.000048	-0.000016
10 H	-0.000025	-0.000094	-0.000016
11 C	0.000049	-0.000083	-0.000067
12 H	0.000001	-0.000057	0.000047
13 C	-0.000064	0.000066	-0.000073
14 C	0.000125	-0.000152	0.000237
15 C	-0.000002	0.000148	0.000008
16 H	0.000052	0.000097	-0.000059
17 C	0.000026	-0.000045	0.000187
18 H	0.000134	0.000103	-0.000107
19 C	0.000012	0.000116	-0.000041
20 H	0.000125	0.000020	-0.000040
21 C	0.000089	-0.000047	0.000017
22 H	0.000080	-0.000051	0.000034
23 C	0.000021	0.000078	-0.000278
24 H	0.000037	-0.000061	0.000076
25 C	-0.000125	-0.000123	-0.000104
26 C	0.000031	0.000023	0.000127
27 C	-0.000049	0.000083	-0.000067
28 H	-0.000001	0.000057	0.000047
29 C	0.000040	0.000048	-0.000016
30 H	0.000025	0.000094	-0.000016
31 C	-0.000009	0.000018	-0.000018
32 H	0.000056	0.000016	-0.000040
33 C	-0.000015	-0.000065	-0.000039
34 H	0.000037	-0.000043	-0.000049
35 C	0.000058	0.000038	-0.000003
36 H	-0.000009	-0.000075	-0.000015
37 C	0.000064	-0.000066	-0.000073
38 C	-0.000125	0.000152	0.000237
39 C	0.000002	-0.000148	0.000008
40 H	-0.000052	-0.000097	-0.000059
41 C	-0.000026	0.000045	0.000187
42 H	-0.000134	-0.000103	-0.000107
43 C	-0.000012	-0.000116	-0.000241
44 H	-0.000125	-0.000020	-0.000040
45 C	-0.000089	0.000047	0.000017
46 H	-0.000080	0.000051	0.000034
47 C	-0.000021	-0.000078	-0.000278
48 H	-0.000037	0.000061	0.000076
49 O	0.000306	0.000286	-0.000013
50 O	-0.000270	0.000107	0.000024
51 O	-0.000306	-0.000286	-0.000013
52 O	0.000270	-0.000107	0.000024
53 S	-0.000208	0.000223	0.000059
54 H	0.000027	-0.000029	0.000045
55 O	0.000000	0.000000	0.000248
56 Co	0.000000	0.000000	0.000448
57 Pt	0.000000	0.000000	-0.000616
58 S	-0.000074	-0.000189	0.000277
59 S	0.000208	-0.000223	0.000059
60 S	0.000074	0.000189	0.0000277
61 H	-0.000027	0.000029	0.000045

Geometry Convergence Tests

Energy old : -14.55458387
new : -14.55459601

Convergence tests:
(Energies in hartree, Gradients in hartree/angstrom or radian, Lengths in angstrom, Angles in degrees)

Item	Value	Criterion	Conv.	Ratio
change in energy	-0.00001214	0.00100000	YES	1.13776998
gradient max	0.00061633	0.00100000	YES	0.59548108
gradient rms	0.00012022	0.00066667	YES	0.68918781
cart. step max	0.00318834	0.01000000	YES	0.92660265
cart. step rms	0.00133089	0.00666667	YES	0.93351353
		hartree	eV	kcal/mol
Pauli Repulsion				
Kinetic (Delta T^0):	163.069104715685910	4437.3361	102327.42	428137.87
Delta V^Pauli Coulomb:	-83.784654089935074	-2279.8964	-52575.67	-219976.58
Delta V^Pauli LDA-XC:	-20.559016856117928	-559.4393	-12900.98	-53977.69
Delta V^Pauli GGA-Exchange:	1.060766532017468	28.8649	665.64	2785.04
Delta V^Pauli GGA-Correlation:	-0.242751809284208	-6.6056	-152.33	-637.34
Total Pauli Repulsion:	59.543448492366167	1620.2597	37364.08	156331.30
(Total Pauli Repulsion = Delta E^Pauli in BB paper)				
Steric Interaction				
Pauli Repulsion (Delta E^Pauli):	59.543448492366167	1620.2597	37364.08	156331.30
Electrostatic Interaction:	-12.656448876219988	-344.3995	-7942.04	-33229.50
(Electrostatic Interaction = Delta V_elstat in the BB paper)				
Total Steric Interaction:	46.886999616146177	1275.8602	29422.04	123101.80
(Total Steric Interaction = Delta E^0 in the BB paper)				
Orbital Interactions				
A:	-30.656225842359717	-834.1983	-19237.07	-80487.91
B:	-30.727841948627120	-836.1471	-19282.01	-80675.94
Total Orbital Interactions:	-61.389292531943077	-1670.4876	-38522.37	-161177.56
Alternative Decomposition Orb.Int.				
Kinetic:	-149.0076667682472800	-4054.7049	-93503.73	-391219.58
Coulomb:	81.224639024448450	2210.2349	50969.24	213255.26
XC:	6.393736126081305	173.9824	4012.13	16786.75
Total Orbital Interactions:	-61.389292531943042	-1670.4876	-38522.37	-161177.56
Residu (E=Steric+OrbInt+Res):	-0.000065305147029	-0.0018	-0.04	-0.17
Dispersion Energy:	-0.052242464768293	-1.4216	-32.78	-137.16
Total Bonding Energy:	-14.554600685712222	-396.0508	-9133.15	-38213.10
Summary of Bonding Energy (energy terms are taken from the energy decomposition above)				
=====	=====	=====	=====	=====
Electrostatic Energy:	-12.656448876219988	-344.3995	-7942.04	-33229.50
Kinetic Energy:	14.061437033213096	382.6312	8823.69	36918.30
Coulomb (Steric+OrbInt) Energy:	-2.560080370633656	-69.6633	-1606.47	-6721.49
XC Energy:	-13.347266007303361	-363.1976	-8375.54	-35043.24
Dispersion Energy:	-0.052242464768293	-1.4216	-32.78	-137.16
Total Bonding Energy:	-14.554600685712202	-396.0508	-9133.15	-38213.10

[NiPt(tba).H₂O], (ZORA) PBE-D3/AE-TZP, C₂ symmetry

Atom	Cartesian (a.u./angstrom)		
	X	Y	Z
1 Pt	0.000000	0.000000	0.000452
2 Ni	0.000000	0.000000	0.000417
3 S	-0.000232	-0.000154	-0.000357
4 S	0.000472	-0.000640	-0.000315
5 O	0.000294	0.000330	0.000029
6 O	-0.000140	-0.000178	0.000039
7 C	-0.000044	0.000127	0.000009
8 C	0.000155	0.000136	-0.000278
9 C	-0.000051	0.000195	0.000056
10 H	0.000134	0.000061	-0.000007
11 C	0.000016	0.000060	0.000175
12 H	0.000082	0.000003	0.000091
13 C	0.000164	0.000001	-0.000178
14 H	0.000018	-0.000019	-0.000067
15 C	-0.000273	0.000233	-0.000066
16 H	-0.000240	-0.000054	0.000081
17 C	0.000075	0.000218	0.000047
18 H	0.000003	-0.000023	-0.000152
19 C	0.000023	0.000066	0.000155
20 O	0.000000	0.000000	-0.000540
21 C	0.000168	-0.000083	-0.000081
22 C	-0.000147	-0.000004	-0.000078
23 H	0.000013	0.000162	0.000057
24 C	-0.000228	0.000080	0.000125
25 H	0.000088	0.000125	0.000078
26 C	0.000010	-0.000010	0.000064
27 H	0.000142	0.000014	0.000234
28 C	-0.000125	-0.000154	-0.000070
29 H	0.000118	-0.000089	0.000085
30 C	0.000096	0.000024	0.000076
31 H	-0.000029	-0.000193	-0.000068
32 H	-0.000252	-0.000254	0.000149
33 H	0.000252	0.000254	0.000149
34 H	-0.000142	-0.000014	0.000234
35 C	0.000125	0.000154	-0.000070
36 H	-0.000118	0.000089	0.000085
37 C	-0.000096	-0.000024	0.000076
38 H	0.000029	0.000193	-0.000068
39 S	0.000232	0.000154	-0.000357
40 S	-0.000472	0.000640	-0.000315
41 O	-0.000294	-0.000330	0.000029
42 O	0.000140	0.000178	0.000039
43 C	0.000044	-0.000127	0.000009
44 C	-0.000155	-0.000136	-0.000278
45 C	0.000051	-0.000195	0.000056
46 H	-0.000134	-0.000061	-0.000007
47 C	-0.000016	-0.000060	0.000175
48 H	-0.000082	-0.000003	0.000091
49 C	-0.000164	-0.000001	-0.000178
50 H	-0.000018	0.000019	-0.000067
51 C	0.000273	-0.000233	-0.000066
52 H	0.000240	0.000054	0.000081
53 C	-0.000075	-0.000218	0.000047
54 H	-0.000003	0.000023	-0.000152
55 C	-0.000023	-0.000066	0.000155
56 C	-0.000168	0.000083	-0.000081
57 C	0.000147	0.000004	-0.000078
58 H	-0.000013	-0.000162	0.000057
59 C	0.000228	-0.000080	0.000125
60 H	-0.000088	-0.000125	0.000078
61 C	-0.000010	0.000010	0.000064

Geometry Convergence Tests

Energy old : -14.46734425
new : -14.46762863

Convergence tests:
(Energies in hartree, Gradients in hartree/angstrom or radian, Lengths in angstrom, Angles in degrees)

Item	Value	Criterion	Conv.	Ratio	
					hartree eV kcal/mol kJ/mol
change in energy	-0.00028437	0.00100000	YES	30.80841036	
gradient max	0.00063427	0.00100000	YES	0.58636591	
gradient rms	0.00017132	0.00066667	YES	0.73276183	
cart. step max	0.00603312	0.01000000	YES	0.86374937	
cart. step rms	0.00197461	0.00666667	YES	0.91255371	
<hr/>					
Pauli Repulsion					
Kinetic (Delta T^0):	162.938982892738181		4433.7953	102245.77	427796.24
Delta V^Pauli Coulomb:	-83.793401363978163		-2280.1345	-52581.16	-219999.54
Delta V^Pauli LDA-XC:	-20.546665375211987		-559.1032	-12893.23	-53945.26
Delta V^Pauli GGA-Exchange:	1.050245174589243		28.5786	659.04	2757.42
Delta V^Pauli GGA-Correlation:	-0.236137893889348		-6.4256	-148.18	-619.98
Total Pauli Repulsion:	59.413023434247926		1616.7106	37282.24	155988.87
(Total Pauli Repulsion = Delta E^Pauli in BB paper)					
<hr/>					
Steric Interaction					
Pauli Repulsion (Delta E^Pauli):	59.413023434247926		1616.7106	37282.24	155988.87
Electrostatic Interaction:	-12.558092255702892		-341.7231	-7880.32	-32971.27
(Electrostatic Interaction = Delta V_elstat in the BB paper)					
Total Steric Interaction:	46.854931178545030		1274.9875	29401.92	123017.60
(Total Steric Interaction = Delta E^0 in the BB paper)					
<hr/>					
Orbital Interactions					
A:	-30.725901678906872		-836.0943	-19280.80	-80670.84
B:	-30.536700420384335		-830.9459	-19162.07	-80174.10
Total Orbital Interactions:	-61.269658685740218		-1667.2322	-38447.30	-160863.47
<hr/>					
Alternative Decomposition Orb.Int.					
Kinetic:	-149.028606839670772		-4055.2747	-93516.87	-391274.55
Coulomb:	81.077769124956603		2206.2384	50877.07	212869.65
XC:	6.681179028973953		181.8041	4192.50	17541.43
Total Orbital Interactions:	-61.269658685740218		-1667.2322	-38447.30	-160863.47
Residu (E=Steric+OrbInt+Res):	-0.000077926500815		-0.0021	-0.05	-0.20
Dispersion Energy:	-0.052914334374964		-1.4399	-33.20	-138.93
Total Bonding Energy:	-14.467719768070967		-393.6867	-9078.63	-37984.99
<hr/>					
Summary of Bonding Energy (energy terms are taken from the energy decomposition above)					
Electrostatic Energy:	-12.558092255702892		-341.7231	-7880.32	-32971.27
Kinetic Energy:	13.910376053067395		378.5206	8728.89	36521.69
Coulomb (Steric+OrbInt) Energy:	-2.715710165522367		-73.8982	-1704.13	-7130.10
XC Energy:	-13.051379065538139		-355.1461	-8189.86	-34266.39
Dispersion Energy:	-0.052914334374964		-1.4399	-33.20	-138.93
Total Bonding Energy:	-14.467719768070967		-393.6867	-9078.63	-37984.99

2a, (ZORA) PBE-D3/AE-TZP, D_2 symmetry

Atom	Cartesian (a.u./angstrom)		
	X	Y	Z
1 Pt	0.000600	0.000000	0.000000
2 Co	0.000137	0.000000	0.000000
3 S	-0.000100	-0.000085	-0.000257
4 S	-0.000071	-0.000061	0.000045
5 O	0.000285	0.000318	-0.000235
6 O	0.000034	-0.000380	-0.000054
7 C	0.000058	0.000077	0.000023
8 C	0.000022	-0.000021	-0.000006
9 C	0.000097	0.000018	0.000004
10 H	0.000018	-0.000007	-0.000027
11 C	0.000187	-0.000004	-0.000044
12 H	0.000053	0.000097	-0.000095
13 C	-0.000043	-0.000046	-0.000179
14 H	0.000077	0.000118	0.000027
15 C	0.000133	0.000057	-0.000020
16 H	0.000095	0.000044	0.000003
17 C	0.000024	0.000023	0.000085
18 H	0.000055	0.000004	-0.000011
19 C	0.000160	0.000090	-0.000016
20 O	0.000193	0.000000	0.000000
21 C	-0.000192	-0.000183	0.000143
22 C	0.000379	-0.000157	0.000057
23 H	-0.000136	0.000047	-0.000025
24 C	-0.000068	0.000405	-0.000018
25 H	-0.000092	-0.000096	-0.000016
26 C	-0.000083	-0.000180	0.000063
27 H	-0.000017	0.000091	-0.000043
28 C	0.000291	-0.000250	0.000056
29 H	-0.000142	0.000032	-0.000104
30 C	-0.000010	0.000372	-0.000080
31 H	-0.000051	-0.000121	0.000031
32 H	-0.000085	-0.000143	-0.000169
33 H	-0.000085	0.000143	0.000169
34 Pt	-0.000600	0.000000	0.000000
35 Co	-0.000137	0.000000	0.000000
36 S	0.000100	0.000085	-0.000257
37 S	0.000071	0.000061	0.000045
38 O	-0.000285	-0.000318	-0.000235
39 O	-0.000034	0.000380	-0.000054
40 C	-0.000058	-0.000077	0.000023
41 C	-0.000022	0.000021	-0.000006
42 C	-0.000097	-0.000018	0.000004
43 H	-0.000018	0.000007	-0.000027
44 C	-0.000187	0.000004	-0.000044
45 H	-0.000053	-0.000097	-0.000095
46 C	0.000043	0.000046	-0.000179
47 H	-0.000077	-0.000118	0.000027
48 C	-0.000133	-0.000057	-0.000020
49 H	-0.000095	-0.000044	0.000003
50 C	-0.000024	-0.000023	0.000085
51 H	-0.000055	-0.000004	-0.000011
52 C	-0.000160	-0.000090	-0.000016
53 O	-0.000193	0.000000	0.000000
54 C	0.000192	0.000183	0.000143
55 C	-0.000379	0.000157	0.000057
56 H	0.000136	-0.000047	-0.000025
57 C	0.000068	-0.000405	-0.000018
58 H	0.000092	0.000096	-0.000016
59 C	0.000083	0.000180	0.000063
60 H	0.000017	-0.000091	-0.000043
61 C	-0.000291	0.000250	0.000056
62 H	0.000142	-0.000032	-0.000104
63 C	0.000010	-0.000372	-0.000080
64 H	0.000051	0.000121	0.000031
65 H	0.000085	0.000143	-0.000169
66 H	0.000085	-0.000143	0.000169
67 S	0.000100	-0.000085	0.000257
68 S	0.000071	-0.000061	-0.000045
69 O	-0.000285	0.000318	0.000235
70 O	-0.000034	-0.000380	0.000054
71 C	-0.000058	0.000077	-0.000023
72 C	-0.000022	-0.000021	0.000006
73 C	-0.000097	0.000018	-0.000004

```

74 H -0.000018 -0.000007 0.000027
75 C -0.000187 -0.000004 0.000044
76 H -0.000053 0.000097 0.000095
77 C 0.000043 -0.000046 0.000179
78 H -0.000077 0.000118 -0.000027
79 C -0.000133 0.000057 0.000020
80 H -0.000095 0.000044 -0.000003
81 C -0.000024 0.000023 -0.000085
82 H -0.000055 0.000004 0.000011
83 C -0.000160 0.000090 0.000016
84 C 0.000192 -0.000183 -0.000143
85 C -0.000379 -0.000157 -0.000057
86 H 0.000136 0.000047 0.000025
87 C 0.000068 0.000405 0.000018
88 H 0.000092 -0.000096 0.000016
89 C 0.000083 -0.000180 -0.000063
90 H 0.000017 0.000091 0.000043
91 C -0.000291 -0.000250 -0.000056
92 H 0.000142 0.000032 0.000104
93 C 0.000010 0.000372 0.000080
94 H 0.000051 -0.000121 -0.000031
95 S -0.000100 0.000085 0.000257
96 S -0.000071 0.000061 -0.000045
97 O 0.000285 -0.000318 0.000235
98 O 0.000034 0.000380 0.000054
99 C 0.000058 -0.000077 -0.000023
100 C 0.000022 0.000021 0.000006
101 C 0.000097 -0.000018 -0.000004
102 H 0.000018 0.000007 0.000027
103 C 0.000187 0.000004 0.000044
104 H 0.000053 -0.000097 0.000095
105 C -0.000043 0.000046 0.000179
106 H 0.000077 -0.000118 -0.000027
107 C 0.000133 -0.000057 0.000020
108 H 0.000095 -0.000044 -0.000003
109 C 0.000024 -0.000023 -0.000085
110 H 0.000055 -0.000004 0.000011
111 C 0.000160 -0.000090 0.000016
112 C -0.000192 0.000183 -0.000143
113 C 0.000379 0.000157 -0.000057
114 H -0.000136 -0.000047 0.000025
115 C -0.000068 -0.000405 0.000018
116 H -0.000092 0.000096 0.000016
117 C -0.000083 0.000180 -0.000063
118 H -0.000017 -0.000091 0.000043
119 C 0.000291 0.000250 -0.000056
120 H -0.000142 -0.000032 0.000104
121 C -0.000010 -0.000372 0.000080
122 H -0.000051 0.000121 -0.000031
-----
```

Geometry Convergence Tests

```

Energy old : -29.13828927
new : -29.13847153

```

Convergence tests:

(Energies in hartree, Gradients in hartree/angstr or radian, Lengths in angstrom, Angles in degrees)

Item	Value	Criterion	Conv.	Ratio
change in energy	-0.00018226	0.00100000	YES	1.79212368
gradient max	0.00059950	0.00100000	YES	0.08345791
gradient rms	0.00014134	0.00066667	YES	0.07420168
cart. step max	0.00225876	0.01000000	YES	0.70658123
cart. step rms	0.00051470	0.00666667	YES	0.38072224

	hartree	eV	kcal/mol	kJ/mol
Pauli Repulsion				
Kinetic (Delta T^0):	328.051962364114956	8926.7481	205855.74	861300.31
Delta V^Pauli Coulomb:	-169.049866555853015	-4600.0809	-106080.40	-443840.36
Delta V^Pauli LDA-XC:	-41.385887185124027	-1126.1673	-25970.04	-108658.63
Delta V^Pauli GGA-Exchange:	2.162736971610599	58.8511	1357.14	5678.27
Delta V^Pauli GGA-Correlation:	-0.503385483868119	-13.6978	-315.88	-1321.64
Total Pauli Repulsion:	119.275560110880392	3245.6531	74846.55	313157.94
(Total Pauli Repulsion =				

Delta E[^]Pauli in BB paper)

Steric Interaction

Pauli Repulsion (Delta E [^] Pauli):	119.275560110880392	3245.6531	74846.55	313157.94
Electrostatic Interaction:	-25.377636472419201	-690.5606	-15924.71	-66628.98
(Electrostatic Interaction =				
Delta V_elstat in the BB paper)				

Total Steric Interaction:	93.897923638461194	2555.0925	58921.84	246528.96
(Total Steric Interaction =				

Delta E⁰ in the BB paper)

Orbital Interactions

A:	-30.676181682871555	-834.7414	-19249.60	-80540.30
B1:	-30.694961900255443	-835.2524	-19261.38	-80589.61
B2:	-30.698667407282684	-835.3532	-19263.71	-80599.34
B3:	-30.821500814822645	-838.6957	-19340.79	-80921.84

Total Orbital Interactions:	-122.907127590847082	-3344.4731	-77125.40	-322692.62
-----------------------------	----------------------	------------	-----------	------------

Alternative Decomposition Orb.Int.

Kinetic:	-299.608304603239390	-8152.7568	-188007.07	-786621.49
Coulomb:	163.685032087350407	4454.0963	102713.92	429754.99
XC:	13.016144925041919	354.1873	8167.76	34173.88

Total Orbital Interactions:	-122.907127590847068	-3344.4731	-77125.40	-322692.62
-----------------------------	----------------------	------------	-----------	------------

Residu (E=Steric+OrbInt+Res):	-0.000168148895142	-0.0046	-0.11	-0.44
Dispersion Energy:	-0.129137095157059	-3.5140	-81.03	-339.05

Total Bonding Energy:	-29.138509196438090	-792.8992	-18284.69	-76503.15
-----------------------	---------------------	-----------	-----------	-----------

Summary of Bonding Energy (energy terms are taken from the energy decomposition above)

Electrostatic Energy:	-25.377636472419201	-690.5606	-15924.71	-66628.98
Kinetic Energy:	28.443657760875567	773.9913	17848.67	74678.81
Coulomb (Steric+OrbInt) Energy:	-5.365002617397749	-145.9891	-3366.59	-14085.81
XC Energy:	-26.710390772339625	-726.8267	-16761.03	-70128.12
Dispersion Energy:	-0.129137095157059	-3.5140	-81.03	-339.05

Total Bonding Energy:	-29.138509196438068	-792.8992	-18284.69	-76503.15
-----------------------	---------------------	-----------	-----------	-----------

3, (ZORA) PBE-D3/AE-TZP, D_2 symmetry

Atom	Cartesian (a.u./angstrom)		
	X	Y	Z
1 Pt	0.000379	0.000000	0.000000
2 Ni	-0.000183	0.000000	0.000000
3 S	0.000065	-0.000099	0.000095
4 S	0.000034	-0.000161	0.000051
5 O	-0.000170	0.000474	-0.000666
6 O	0.000266	-0.000645	-0.000717
7 C	-0.000099	-0.000004	0.000396
8 C	0.000168	0.000047	0.000137
9 C	-0.000147	0.000114	0.000041
10 H	0.000094	0.000091	-0.000036
11 C	0.000091	-0.000134	0.000174
12 H	-0.000011	0.000046	-0.000104
13 C	-0.000125	0.000046	0.000016
14 H	-0.000098	-0.000001	0.000066
15 C	-0.000023	0.000338	0.000322
16 H	-0.000103	-0.000164	0.000194
17 C	-0.000061	-0.000154	-0.000403
18 H	-0.000070	-0.000023	-0.000101
19 C	0.000059	-0.000054	0.000159
20 O	-0.000116	0.000000	0.000000
21 C	0.000113	0.000036	-0.000067
22 C	-0.000014	0.000203	-0.000066
23 H	0.000107	-0.000070	-0.000188
24 C	0.000001	-0.000017	-0.000015
25 H	-0.000013	0.000013	0.000051
26 C	-0.0000132	-0.000021	-0.000059
27 H	-0.000098	0.000065	0.000149
28 C	0.0000100	0.000018	-0.000299
29 H	-0.000165	0.000035	0.000108
30 C	-0.0000204	-0.000041	0.000071
31 H	-0.000069	-0.000145	-0.000229
32 H	0.000022	-0.000336	0.000014
33 H	0.000022	0.000336	-0.000014
34 Pt	-0.000379	0.000000	0.000000
35 Ni	0.000183	0.000000	0.000000
36 S	-0.000065	0.000099	0.000095
37 S	-0.000034	0.000161	0.000051
38 O	0.000170	-0.000474	-0.000666
39 O	-0.000266	0.000645	-0.000717
40 C	0.000099	0.000004	0.000396
41 C	-0.000168	-0.000047	0.000137
42 C	0.000147	-0.000114	0.000041
43 H	-0.000094	-0.000091	-0.000036
44 C	-0.000091	0.000134	0.000174
45 H	0.000011	-0.000046	-0.000104
46 C	0.000125	-0.000046	0.000016
47 H	0.000098	0.000001	0.000066
48 C	0.000023	-0.000338	0.000322
49 H	0.000103	0.000164	0.000194
50 C	0.000061	0.000154	-0.000403
51 H	0.000070	0.000023	-0.000101
52 C	-0.000059	0.000054	0.000159
53 O	0.000116	0.000000	0.000000
54 C	-0.000013	-0.000036	-0.000067
55 C	0.000014	-0.000203	-0.000066
56 H	-0.0000107	0.000070	-0.000188
57 C	-0.000001	0.000017	-0.000015
58 H	0.000013	-0.000013	0.000051
59 C	0.0000132	0.000021	-0.000059
60 H	0.000098	-0.000065	0.000149
61 C	-0.000100	-0.000018	-0.000299
62 H	0.000165	-0.000035	0.000108
63 C	0.0000204	0.000041	0.000071
64 H	0.000069	0.000145	-0.000229
65 H	-0.000022	0.000336	0.000014
66 H	-0.000022	-0.000336	-0.000014
67 S	-0.000065	-0.000099	-0.000095
68 S	-0.000034	-0.000161	-0.000051
69 O	0.000170	0.000474	0.000666
70 O	-0.000266	-0.000645	0.000717
71 C	0.000099	-0.000004	-0.000396
72 C	-0.000168	0.000047	-0.000137
73 C	0.000147	0.000114	-0.000041
74 H	-0.000094	0.000091	0.000036

```

75 C -0.000091 -0.000134 -0.000174
76 H 0.000011 0.000046 0.000104
77 C 0.000125 0.000046 -0.000016
78 H 0.000098 -0.000001 -0.000066
79 C 0.000023 0.000338 -0.000322
80 H 0.000103 -0.000164 -0.000194
81 C 0.000061 -0.000154 0.000403
82 H 0.000070 -0.000023 0.000101
83 C -0.000059 -0.000054 -0.000159
84 C -0.000113 0.000036 0.000067
85 C 0.000114 0.000203 0.000066
86 H -0.000107 -0.000070 0.000188
87 C -0.000001 -0.000017 0.000015
88 H 0.000013 0.000013 -0.000051
89 C 0.000132 -0.000021 0.000059
90 H 0.000098 0.000065 -0.000149
91 C -0.000100 0.000018 0.000299
92 H 0.000165 0.000035 -0.000108
93 C 0.000204 -0.000041 -0.000071
94 H 0.000069 -0.000145 0.000229
95 S 0.000065 0.000099 -0.000095
96 S 0.000034 0.000161 -0.000051
97 O -0.000170 -0.000474 0.000666
98 O 0.000266 0.000645 0.000717
99 C -0.000099 0.000004 -0.000396
100 C 0.000168 -0.000047 -0.000137
101 C -0.000147 -0.000114 -0.000041
102 H 0.000094 -0.000091 0.000036
103 C 0.000091 0.000134 -0.000174
104 H -0.000011 -0.000046 0.000104
105 C -0.000125 -0.000046 -0.000016
106 H -0.000098 0.000001 -0.000066
107 C -0.000023 -0.000338 -0.000322
108 H -0.000103 0.000164 -0.000194
109 C -0.000061 0.000154 0.000403
110 H -0.000070 0.000023 0.000101
111 C 0.000059 0.000054 -0.000159
112 C 0.000113 -0.000036 0.000067
113 C -0.000114 -0.000203 0.000066
114 H 0.000107 0.000070 0.000188
115 C 0.000001 0.000017 0.000015
116 H -0.000013 -0.000013 -0.000051
117 C -0.000132 0.000021 0.000059
118 H -0.000098 -0.000065 -0.000149
119 C 0.000100 -0.000018 0.000299
120 H -0.000165 -0.000035 -0.000108
121 C -0.000204 0.000041 -0.000071
122 H -0.000069 0.000145 0.000229
-----
```

Geometry Convergence Tests

```

Energy old : -28.95253226
new : -28.95307647

```

Convergence tests:
 (Energies in hartree, Gradients in hartree/angstr or radian, Lengths in angstrom, Angles in degrees)

Item	Value	Criterion	Conv.	Ratio
change in energy	-0.00054421	0.00100000	YES	1.37317542
gradient max	0.00071707	0.00100000	YES	0.67777505
gradient rms	0.00019043	0.00066667	YES	0.88952227
cart. step max	0.00746248	0.01000000	YES	0.67227856
cart. step rms	0.00171843	0.00666667	YES	0.76349154

	hartree	eV	kcal/mol	kJ/mol
Pauli Repulsion				
Kinetic (Delta T^0):	328.371135898023169	8935.4332	206056.02	862138.30
Delta V^Pauli Coulomb:	-169.513891041223900	-4612.7077	-106371.58	-445058.66
Delta V^Pauli LDA-XC:	-41.440827155138621	-1127.6623	-26004.51	-108802.88
Delta V^Pauli GGA-Exchange:	2.150327043409050	58.5134	1349.35	5645.68
Delta V^Pauli GGA-Correlation:	-0.495292544298014	-13.4776	-310.80	-1300.39
Total Pauli Repulsion:	119.071452200771688	3240.0991	74718.47	312622.05
(Total Pauli Repulsion = Delta E^Pauli in BB paper)				

Steric Interaction				
Pauli Repulsion (Delta E^Pauli):	119.071452200771688	3240.0991	74718.47	312622.05
Electrostatic Interaction:	-25.212611200831169	-686.0701	-15821.15	-66195.70
(Electrostatic Interaction =				
Delta V_elstat in the BB paper)				
-----	-----	-----	-----	-----
Total Steric Interaction:	93.858840999940526	2554.0290	58897.32	246426.35
(Total Steric Interaction =				
Delta E^0 in the BB paper)				
Orbital Interactions				
A:	-30.850024228674368	-839.4719	-19358.68	-80996.73
B1:	-30.504711855987480	-830.0754	-19142.00	-80090.11
B2:	-30.508376011042749	-830.1752	-19144.30	-80099.73
B3:	-30.792687883281786	-837.9117	-19322.71	-80846.19
-----	-----	-----	-----	-----
Total Orbital Interactions:	-122.679680140682990	-3338.2839	-76982.67	-322095.45
Alternative Decomposition Orb.Int.				
Kinetic:	-300.219382104363660	-8169.3850	-188390.53	-788225.88
Coulomb:	163.820797731790719	4457.7907	102799.11	430111.44
XC:	13.718904231889965	373.3104	8608.74	36018.98
-----	-----	-----	-----	-----
Total Orbital Interactions:	-122.679680140682976	-3338.2839	-76982.67	-322095.45
Residu (E=Steric+OrbInt+Res):	-0.000221824651469	-0.0060	-0.14	-0.58
Dispersion Energy:	-0.131726425425834	-3.5845	-82.66	-345.85
Total Bonding Energy:	-28.952787390819765	-787.8454	-18168.15	-76015.53
Summary of Bonding Energy (energy terms are taken from the energy decomposition above)				
=====	=====	=====	=====	=====
Electrostatic Energy:	-25.212611200831169	-686.0701	-15821.15	-66195.70
Kinetic Energy:	28.151753793659509	766.0482	17665.49	73912.42
Coulomb (Steric+OrbInt) Energy:	-5.693315134084656	-154.9230	-3572.61	-14947.80
XC Energy:	-26.066888424137620	-709.3161	-16357.22	-68438.61
Dispersion Energy:	-0.131726425425834	-3.5845	-82.66	-345.85
-----	-----	-----	-----	-----
Total Bonding Energy:	-28.952787390819772	-787.8454	-18168.15	-76015.53

References:

1. G. B. Kauffman, *Inorg. Synth.*, 1967, **9**, 182-185.
2. R. N. Keller, *Inorg. Synth.*, 1946, **2**, 247-250.
3. G. B. Kauffman, *Inorg. Synth.*, 1963, **7**, 239-244.
4. G. A. Melson, N. P. Crawford and B. J. Geddes, *Inorg. Chem.*, 1970, **9**, 1123-1126.
5. *Amsterdam Density Functional*, (2003) Department of Theoretical Chemistry, Vrije Universiteit Amsterdam, The Netherlands.
6. C. Fonseca Guerra, J. G. Snijders, G. te Velde and E. J. Baerends, *Theor. Chem. Acc.*, 1998, **99**, 391-403.
7. E. J. Baerends, T. Ziegler, J. Autschbach, D. Bashford, A. Bérçes, F. M. Bickelhaupt, C. Bo, P. M. Boerrigter, L. Cavallo, D. P. Chong, L. Deng, R. M. Dickson, D. E. Ellis, M. v. Faassen, L. Fan, T. H. Fischer, C. F. Guerra, A. Ghysels, A. Giammona, S. J. A. v. Gisbergen, A. W. Götz, J. A. Groeneveld, O. V. Gritsenko, M. Grüning, S. Gusarov, F. E. Harris, P. v. d. Hoek, C. R. Jacob, H. Jacobsen, L. Jensen, J. W. Kaminski, G. v. Kessel, F. Kootstra, A. Kovalenko, M. V. Krykunov, E. v. Lenthe, D. A. McCormack, A. Michalak, M. Mitoraj, J. Neugebauer, V. P. Nicu, L. Noodleman, V. P. Osinga, S. Patchkovskii, P. H. T. Philipsen, D. Post, C. C. Pye, W. Ravenek, J. I. Rodríguez, P. Ros, P. R. T. Schipper, G. Schreckenbach, J. S. Seldenthuis, M. Seth, J. G. Snijders, M. Solà, M. Swart, D. Swerhone, G. t. Velde, P. Vernooij, L. Versluis, L. Visscher, O. Visser, F. Wang, T. A. Wesolowski, E. M. v. Wezenbeek, G. Wiesnekker, S. K. Wolff, T. K. Woo and A. L. Yakovlev, *ADF2010*, (2010) SCM, Vrije Universiteit.
8. A. D. Becke, *Phys. Rev. A*, 1988, **38**, 3098-3100
9. C. Lee, W. Yang and R. G. Parr, *Phys. Rev. B*, 1988, **37**, 785-789.
10. J. P. Perdew, K. Burke and M. Ernzerhof, *Phys. Rev. Lett.*, 1996, **77**, 3865-3868.
11. S. Grimme, *WIREs Comp. Mol. Sci.*, 2011, **1**, 211-228.
12. S. Grimme, J. Antony, S. Ehrlich and H. Krieg, *J. Chem. Phys.*, 2010, **132**, 154104.
13. J. P. Perdew and Y. Wang, *Phys. Rev. A*, 1992, **B 45** 13244 -13249.
14. S. D. Vosko, L. Wilk and M. Nusair, *Can. J. Chem.*, 1990, **58**, 1200-1211.
15. D. E. C. Ferreira, W. B. D. Almeida, A. Neves and W. R. Rocha, *Int. J. Quant. Chem.*, 2010, **110**, 1048-1055.
16. E. A. A. Noh and J. Zhang, *Chem. Phys.*, 2006, **330**, 82-89.
17. E. vanLenthe, A. Ehlers and E.-J. Baerends, *J. Chem. Phys.*, 1999, **110**, 8943-8953.
18. E. vanLenthe and E. J. Baerends, *J. Comp. Chem.*, 2003, **24**, 1142-1156.
19. M. S. Gopinathan and K. Jug, *Theoret. Chim. Acta*, 1983, **63**, 497-509.
20. L. Noodleman and E. J. Baerends, *J. Am. Chem. Soc.*, 1984, **106**, 2316-2327.
21. L. Noodleman, D. A. Case and A. Aizman, *J. Am. Chem. Soc.*, 1988, **110**, 1001-1005.
22. T. Soda, Y. Kitagawa, T. Onishi, Y. Takano, Y. Shigeta, H. Nagao, Y. Yoshioka and K. Yamaguchi, *Chem. Phys. Lett.*, 2000, **319**, 223-230.
23. F. Neese, *J. Phys. Chem. Solids*, 2004, **65**, 781-785.
24. K. Boguslawski, C. R. Jacob and M. Reiher, *J. Chem. Theory Comput.*, 2011, **7**, 2740-2752.
25. J. Tao, J. P. Perdew, V. N. Staroverov and G. E. Scuseria, *Phys. Rev. Lett.*, 2003, **91**, 146401-146404.
26. F. Furche and J. P. Perdew, *J. Chem. Phys.*, 2006, **124**, 044103-044127.
27. J. Poater, M. Sola, A. Rimola, L. Rodriguez-Santiago and M. Sodupe, *J. Phys. Chem. A*, 2004, **108**, 6072-6078.
28. L. Grajciar, O. Bludsky and P. Nachtigall, *J. Phys. Chem. Lett.*, 2010, **1**, 3354-3359.
29. M. Ernzerhof and G. Scuseria, *J. Chem. Phys.*, 1999, **110**, 5029-5036.
30. C. Adamo and V. Barone, *J. Chem. Phys.*, 1999, **110**, 6158-6170.

31. P. R. Varadwaj, I. Cukrowski and H. M. Marques, *J. Phys. Chem. A*, 2008, **112**, 10657-10666.
32. R. S. Hunter and R. W. Harold, *The Measurement of Appearance*, Wiley-Interscience, 1987.
33. P. Kubelka and F. Munk, *Z. Tech. Phys.*, 1931, **12**, 593.
34. E. Bill, *julX*, (2008 (http://ewww.mpi-muelheim.mpg.de/bac/logins/bill/julX_en.php)) Max Planck Institute for Bioinorganic Chemistry, Mulheim an der Ruhr.
35. M. P. Shores, J. J. Sokol and J. R. Long, *J. Am. Chem. Soc.*, 2002, **124**, 2279-2292.
36. H. Sakiyama, *MagSaki*, (2007) Sakiyama Laboratory.
37. M. J. Hossain, M. Yamasaki, M. Mikuriya, A. Kurabayashi and H. Sakiyama, *Inorg. Chem.*, 2002, **41**, 4058-4062.
38. A. Rodriguez, H. Sakiyama, N. Masciocchi, S. Galli, N. Gálvez, F. Lloret and E. Colacio, *Inorg. Chem.*, 2005, **44**, 8399-8406.
39. H. Sakiyama, *Inorg. Chim. Acta*, 2006, **359**, 2097-2100.
40. H. Sakiyama, *Inorg. Chim. Acta*, 2007, **360**, 715-716.
41. H. Sakiyama, R. Ito, H. Kumagai, K. Inoue, M. Sakamoto, Y. Nishida and M. Yamasaki, *Eur. J. Inorg. Chem.*, 2001, **2001**, 2027-2032.
42. H. Sakiyama, R. Ito, H. Kumagai, K. Inoue, M. Sakamoto, Y. Nishida and M. Yamasaki, *Eur. J. Inorg. Chem.*, 2001, **2001**, 2705-2705.
43. J. M. Herrera, A. Bleuzen, Y. Dromzée, M. Julve, F. Lloret and M. Verdaguera, *Inorg. Chem.*, 2003, **42**, 7052-7059.
44. L. M. Toma, R. Lescouezec, J. Pasan, C. Ruiz-Perez, J. Vaissermann, J. Cano, R. Carrasco, W. Wernsdorfer, F. Lloret and M. Julve, *J. Am. Chem. Soc.*, 2006, **128**, 4842-4853.